


REVIEW

The CA2 hippocampal subfield in humans: A review

Ricardo Insausti¹ | Monica Muñoz-López¹  | Ana Maria Insausti^{1,2}

¹Human Neuroanatomy Laboratory, and Neuromax Associated Unit CSIC (Spain), Department of Health Sciences, School of Medicine, University of Castilla-La Mancha, Albacete, Spain

²Anatomy Unit, Department of Medical Sciences, School of Health Sciences, Public University of Navarra, Pamplona, Navarra, Spain

Correspondence

Ricardo Insausti, Human Neuroanatomy Laboratory, Department of Health Sciences, School of Medicine, University of Castilla-La Mancha, Almansa 14, 02008 Albacete, Spain. Email: ricardo.insausti@uclm.es

Funding information

National Institutes of Health, Grant/Award Number: R01 AG056014; Universidad de Castilla-La Mancha, Grant/Award Number: 2020-GRIN-28837

Abstract

CA2 is probably the most enigmatic of the hippocampal fields. It is small in size (in humans about 500 μm across the mediolateral axis), and yet, it is involved in important functions, such as in social memory and anxiety. This study offers a glimpse of several significant aspects of the anatomical organization of CA2. We present an overview of the anatomical structure of CA2, imbued in the general organization of the human hippocampal formation. The location and distinctiveness of CA2 is presented in relation with CA3 and CA1, based in a total of 23 human control cases serially sectioned throughout the whole longitudinal axis of the hippocampus, examined every 500 μm in Nissl-stained sections. The longitudinal extent of CA2 is close to 30 mm, starting in the hippocampal head, 2.5 mm caudal to the DG and 3.5 mm caudal to the start of CA3, approximately 10 mm from the hippocampus rostral end. The connective information of human CA2 is very scarce, thereby we relied on nonhuman primate tract tracing studies of the hippocampal formation, given its resemblance to the human brain. Human CA2 is subject of neuropathological studies, and we chose to present Alzheimer's disease, schizophrenia, and Mesial Temporal Lobe Epilepsy with hippocampal sclerosis in those aspects that impinge directly into CA2.

KEYWORDS

anatomy, CA2, hippocampus, memory

1 | HIPPOCAMPAL FORMATION

The Hippocampal Formation (HF) is a functional unit that supports key functions in humans and animals, most notably episodic-like memory and spatial navigation and learning. Anatomically, the HF is part of the medial temporal lobe in all mammal species, close to the adjoining cerebral cortex, through which much of its connections are carried in and out. The HF includes additional anatomically and functionally distinct areas on top of the hippocampus proper. The term hippocampus or hippocampus proper, is applied to the CA subfields (Insausti & Amaral, 2012). The HF includes different cytoarchitectonically fields, with shared characteristics. One of these features is that the layers of HF are organized as primitive cortex in one single cell layer. This

organization receives the name of the *allocortex*. The Dentate Gyrus (DG) is the highlighted feature of the HF. The DG can be seen in unstained coronal sections even without microscope; with the naked eye, occupies its deepest field within the HF. The DG is surrounded by the unfolding hippocampal fields CA3, CA2, CA1 and more medially located, the Subiculum. As the unfolding continues we find the Presubiculum, Parasubiculum, and entorhinal cortex, with an increasing number of layers. The last three fields are referred as *periallocortex*, which are not only different in their cytoarchitecture from the other HF subareas, but they are anatomically connected with different cortical and subcortical brain regions. The Entorhinal cortex (EC), is the most external part of the HF, in the cortical surface of the parahippocampal gyrus of the medial temporal cortex, immediately

This is an open access article under the terms of the [Creative Commons Attribution](https://creativecommons.org/licenses/by/4.0/) License, which permits use, distribution and reproduction in any medium, provided the original work is properly cited.

© 2023 The Authors. *Hippocampus* published by Wiley Periodicals LLC.

adjacent to the perirhinal cortex. The number of layers in the perirhinal and parahippocampal cortices increases, but still has limbic appearance, with slightly primitive laminar organization and it is referred as *proisocortex*. The proisocortex is bounded by the well established 6-layered isocortex or *neocortex*.

This group of heterogenous HF structures are a key part of the limbic memory system in connection with the cortex outside the EC and the diencephalon. Connectivity is a key point in this system. On the one hand, the EC has heavy reciprocal connections with cortical association areas in such a way it is considered the gateway of multiple polysensory cortices and subcortical connections to the hippocampus proper (DG, CA3, CA2, CA1, and Subiculum; Insausti & Amaral, 2012; Insausti et al., 2017). The entorhinal cortex leads cortical association input to the consecutive stages within the HF (Insausti et al., 1987a, 1987b; Insausti & Amaral, 2008). The HF is characterized by a series of unidirectional connections originated in the EC. These connections innervate the DG and hippocampal fields, in a stepwise fashion. This intrinsic hippocampal pathway start is neurons in layer II and VI of the entorhinal cortex that project to the dentate gyrus (DG) and CA3-CA2, while layers III and V project to CA1 and the subiculum (Witter & Amaral, 1991). The DG projects to CA3, which in turn does so to CA2 and CA1 through Schaffer's collaterals; CA2 also projects to the deep part of CA1 (Kohara et al., 2014). Field CA1 projects to both subiculum and deep layers of the entorhinal cortex, from which originate projections back to cortical association areas (Munoz & Insausti, 2005). In parallel, the Subiculum projects to the Presubiculum and Parasubiculum, and those innervate superficial layers of the entorhinal cortex. The deep layers of the EC channel in a very organized way the HF output to multimodal areas distributed in the cerebral cortex.

In sum, the HF is formed by a loop of successive steps in the flow of neural information. The starting point is the entorhinal cortex as it represents the nexus between cortical association areas and the hippocampus, both at the entry and the exit of the set of HF connections. The HF loop of connections is at the core of the limbic memory system.

2 | DEFINITION: WHAT IS AND WHAT IS NOT CA2?

The hippocampal subfield CA2 is one of the components of the HF in humans and other mammals, extends along the rostrocaudal axis of the hippocampus, and it is located between the hippocampal subfields CA3 and CA1 (Insausti & Amaral, 2012).

2.1 | Classical definition of CA2

Rafael Lorente de Nó (Lorente de Nó, 1934) introduced the acronym CA (for *Cornu Ammonis*) to name the different hippocampal subfields. He used the term CA4 for the area closest to the DG (we include CA4 as a part of CA3 field of the hippocampus, see Insausti &

Amaral, 2012). The set of CA fields (CA3, CA2, and CA1) can be distinguished according with the neuronal size of the principal pyramidal cell layer. The pyramidal cell layer in both CA3 and CA2 is characterized by larger neuronal size compared with that in CA1. This feature has often prompted the combination of CA2 and CA3 in a fused field, (i.e., in stereological determinations of the neuron number in CA2-CA3, see below). This feature was noticed by Ramón y Cajal (Ramon y Cajal, 1904), who distinguished a combined CA3 and CA2 field that he called *Regio inferior*, while a small cell layer corresponding to CA1, was called *Regio superior*.

Cornu Ammonis field 2 of Lorente de Nó, (Lorente de Nó, 1934), more commonly named simply as CA2, is one of the allocortical fields of the hippocampus proper, located between CA3 (proximally) and CA1 (distally), and this has been like this during phylogeny. First described in Golgi preparations by Ramón y Cajal (Ramon y Cajal, 1904) and (Lorente de Nó, 1934), CA2 is usually distinguished from the adjacent field CA3 by the lack of the mossy fiber projection from the dentate gyrus granule cell layer. This projection is characterized by the presence of thick dendritic spines (thorny excrescences) in CA3, absent in CA2. Despite this robust criterion for considering CA2 as a distinct hippocampal subfield, that is, independent of CA3, a clear CA2-CA3 separation has long been controversial (Stephan, 1975; von Economo & Koskinas, 1925) and still remains unclear. Nevertheless, the presence of thorny excrescences, distinctive of CA2, is precise and unquestionable, at least in humans. In rodents however, these criteria has been questioned given the identification of the thorny pyramidal cells observed in the CA3 region (Hunt et al., 2018) and the direct innervation of a subset of CA2 pyramidal cells by mossy fibers (Fernandez-Lamo et al., 2019; Kohara et al., 2014). Besides, the presence of mossy fibers in CA2 call for a redefinition of its boundaries by the use of the specific antibodies, RSG14 and PCP4 (Radzicki et al., 2023).¹ Information about structure and organization of CA2 in humans comes from more classical neuroanatomical methods, thereby the more modern molecular neuroanatomy used in experimental species is virtually nonexistent (except for Squires et al., 2018).

The molecular characterization of CA2 is poorly understood, thereby most specialized books still adhere to the classical definition of CA2 hippocampal field, that is, big neurons in the principal cell layer and absence of thorny excrescences in the mossy fiber projection, restricted to the *Stratum lucidum*. However, Squires et al. (2018) reports immunoreactivity to RGS14 in human and nonhuman primates beyond the hippocampus. In that study, immunohistochemical demonstration of RSG14 is described equally in terms of density in CA1 and CA2, but not in CA3 or the DG. Interestingly, RSG14 immunoreactivity

¹The distal termination of the mossy fiber projection lacks an absolute value as boundary between CA3 and CA2, as it has been shown that the granule cell layer of the DG sends projections to CA2, thus extending the mossy fibers beyond CA3, to enter *Stratum radiatum* of CA2. Interestingly, they form synapses as simple spines (thus lacking the big thorny excrescences typical of mossy fiber synapses in CA3); synapses are established in the shaft and apical dendrites of CA2. The increase in width, defined by PCP4-positive cells is about 300 μm relative to the 100 μm by classical anatomical definition (Kohara et al., 2014). In rat, there is a subset of molecularly defined CA2 pyramidal cells (named proximal CA2) directly innervated by the mossy fibers, while the distal subset is lacking such inputs (Fernandez-Lamo et al., 2019). This may suggest important differences between species which are worth to consider in future studies.

seems restricted heavily in pyramidal neurons and dendritic extensions throughout the rostrocaudal extent of the hippocampus. Although CA1 is also rich in immunoreactivity, it is mainly in the neuropil and not in the principal cells (Squires et al., 2018). Like in nonhuman primates, the presence of RSG14 in the human brain is localized in CA2 and CA1, while CA3 seems devoid of labeling. No data exist on the rostrocaudal extent of RSG14 immunoreactivity in humans, probably due to the small hippocampal sample size prepared for paraffin processing (Squires et al., 2018).

Unlike in the rodent, anatomical data on the human CA2 field comes more often from classical anatomical studies. For example, Golgi-stained material (Lauer & Senitz, 2006) or intracellular stain (Benavides-Piccione et al., 2020) confirms the anatomical structure of CA2 in humans, although limited to a small portion of the hippocampal axis. Cell body stains such as Nissl hardly demonstrate the presence of the mossy fiber projection, however, it shows a clear space occupied by mossy fibers in the *Stratum lucidum* ending at the distal end of CA3, and typically restricted to CA3. It is worth noting that in classical terminology, *Stratum lucidum* only applies to CA3, as it is a descriptive term that means translucent appearance of bundles of fibers, often visible macroscopically in the unfixed brain. That concentration of fibers is not noticeable in CA2, thus the name of *Stratum lucidum* is only applied to CA3. In the mouse, and probably in other mammal species as well, however, the criterion of mossy fiber extent applied only to CA3 is not valid any longer.

In sum, while in primates' CA1 pyramidal cell layer is made up by small neurons, CA3 contains larger pyramids and mossy fiber distribution and CA2 is characterized by large pyramidal neurons and mossy fiber input, although without the thorny excrescences characteristic of CA3. The DG innervation of CA2 needs to be confirmed in other species beyond rodents as well as in humans. The new CA2 genetic markers RGS14, PCP4, and STEP help bring together classical and

modern molecular definitions of this important hippocampal region by defining more precise boundaries (Caruana et al., 2012; Fernandez-Lamo et al., 2019; Jones & McHugh, 2011; Lein et al., 2005; Piskorowski & Chevaleyre, 2012). However, to the best of our knowledge, there is no data about the correspondence of classical delimitation (Lauer & Senitz, 2006) with genetic markers in CA2 for human brain. Therefore, it cannot be ruled out that new boundaries of human CA2 hippocampal subfield may or may not be in strict concordance with classical delimitations.

2.2 | Laminar structure of CA2

Like in other hippocampal subfields, the principal cell layer of CA2 is the pyramidal cell layer (Figure 1). The pyramidal cell layer occupies the very center of every CA field of the hippocampus, whereas the other layers surround it. From superficial (closer to the alveus-fimbria) to deep layers (closer to surface of the lateral ventricle), and in a similar fashion to CA3 and CA1, CA2 is first made up of the *Alveus*. Figure 2 shows the CA2 layers, drawn on a histological section of the hippocampus at mid rostro-caudal level. Immediately deep to the alveus lies the *Stratum oriens*, which contains a multiplicity of interneurons. Deep to this stratum, the *Stratum pyramidale*, contains the cell bodies of the principal cells and interneurons. The *Stratum radiatum* contains the apical dendrites from the principal neurons. The deepest stratum, and closest to the hippocampal fissure is the *Stratum lacunosum-moleculare*, directly adjacent to the hippocampal fissure, which contains the terminals from the projections coming from the entorhinal cortex (perforant pathway), as well as other types of extrinsic connections.

Over 20 types of interneurons can be found in addition to pyramidal cells in all the hippocampal subfields, including CA2. Details can

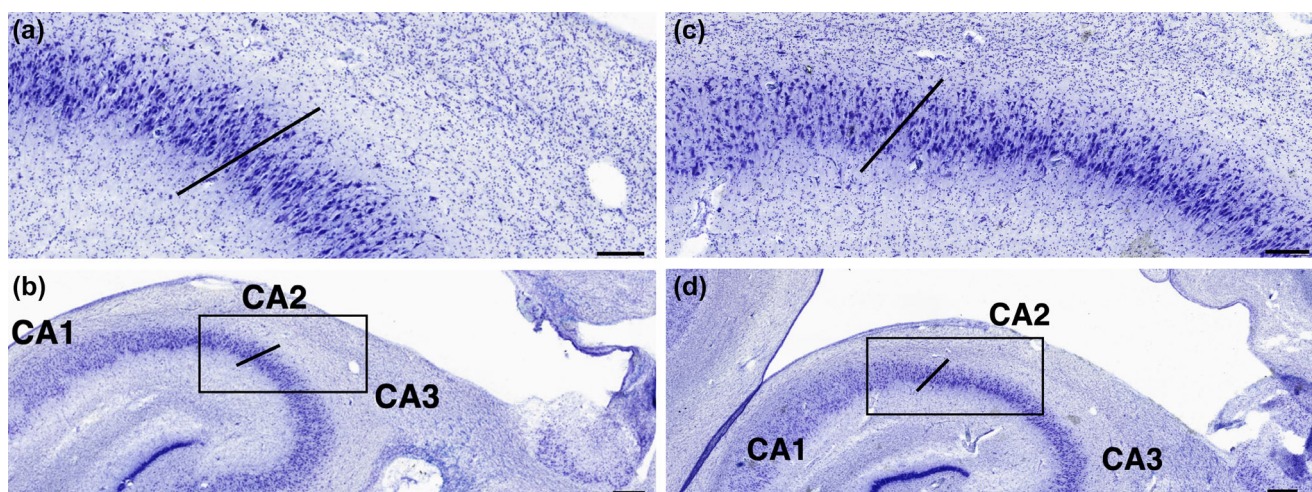


FIGURE 1 Photomicrographs of Nissl stained coronal sections through the hippocampal body illustrate the boundaries of CA2 with adjacent subfields CA2 and CA3 at two different rostro-caudal levels. (a) Boundary between CA2 and CA3 (line, see text for details) indicated in the higher power photomicrograph from the rectangle in B. (b) Lower power photomicrograph illustrates the border between CA1 and CA2 from the rectangle in C. (c) Transition between CA2 to CA1 (line). Note the smaller size of pyramidal neurons in CA2 relative to CA1. (d) Lower power magnification of the field shown in C (rectangle). Scale bar is 200 μ m in A and C, and 500 μ m in B and D.

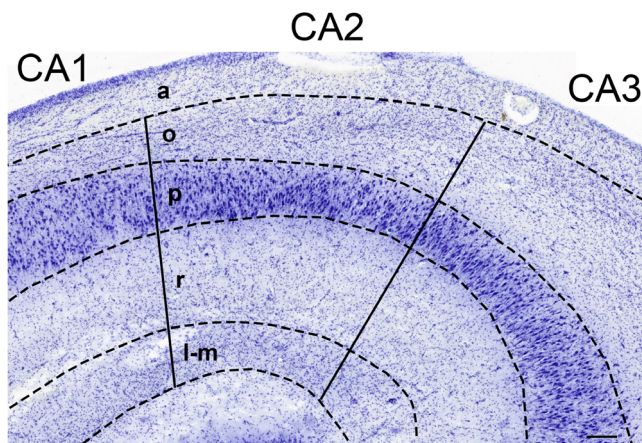


FIGURE 2 Coronal section through the middle of the body of the hippocampus illustrates the stratification in layers of CA2 in the human brain. The outer part corresponds to the alveus and the innermost region to the hippocampal fissure and adjacent molecular layer of the DG (the latter not shown in the figure). a, Alveus; o, Stratum oriens; p, Stratum pyramidale; r, Stratum radiatum; l-m, Stratum lacunosum-moleculare. Radial lines indicate the boundaries with CA3 and CA1.

be revised in Freund and Buzsáki (1996), Booker and Vida (2018), and Insausti and Amaral (2012). In contrast to rodents (Botcher et al., 2014), information about type and distribution of interneurons in CA2 subfield in the human brain is poor, with scattered descriptions of some interneurons immunoreactive to different antigens such as calretinin (Nitsch & Ohm, 1995), calbindin and parvalbumin (Seress et al., 1993).

3 | HIPPOCAMPAL SUBFIELD CA2 CONNECTIVITY

3.1 | Intrinsic hippocampal connectivity of CA2

Data on the intrinsic CA2 connectivity comes from experimental studies in animals, mainly rodents. There are only few studies that examine CA2 anatomical structure in non-human primates and humans, and even less that deal with its connectivity, thereby CA2 intrinsic or extrinsic connectivity is virtually unknown.

Much of the synaptic input of CA2 is intrinsic, that is, it originates and terminates within the hippocampal formation. Neurons in CA2 generate a dense and diffuse plexus of collaterals to CA1, with a less clear topography compared with CA3. Intracellular studies show that CA2 sends collaterals to distal CA3 (Swanson et al., 1978). In addition, data in rodents indicate that CA2 is rich in associational and commissural connections. CA2 axon collaterals terminate more within CA2 Stratum oriens than in the Stratum radiatum, mostly on the ipsilateral side (Shinohara et al., 2012). Also, CA2 projects to the homotopic, contralateral CA2, as well as to the lateral septal nucleus. A small projection to the polymorphic cell layer of the dentate gyrus also arises from CA2 (Scharfman, 2007; Tamamaki et al., 1988), although its function is yet unknown.

3.2 | EC afferents to CA2. Nonhuman primates

In line with the framework of the anatomical organization of the HF exposed above, one of the main inputs to CA2 originates in EC layers II and, to a lesser extent, in layer VI (Witter & Amaral, 1991). This input terminates throughout the Stratum lacunosum-moleculare. However, rostral and caudal EC subareas project differently to CA2. Rostral EC reaches primarily the rostral part of the hippocampus (CA3-CA2), especially at the level of the end of the uncus and beginning of the body of the hippocampus. The caudal part of the uncus receives the heaviest rostral EC projection in CA3-CA2. At midlevel EC projects heavily to CA2, but it does so predominantly towards the caudal part of the hippocampus. The caudal divisions of EC send only weak projections to the CA2-CA3 region, and they concentrate closer to the Stratum radiatum than those from rostral divisions. A mediolateral gradient of the EC projections to CA2 is less obvious, although lateral EC projects somewhat more heavily to the outer portion of Stratum lacunosum-moleculare, while caudal EC does so on its inner portion. In summary, it seems that the heaviest EC projection to CA2 originates at mid-levels of the EC.

3.3 | EC afferents to CA2: Rodents

One of the main inputs to CA2 comes from the EC, which terminates on distal dendrites of pyramidal neurons and interneurons in the Stratum lacunosum-moleculare. EC afferents to CA2 originate from reelin-positive, layer II neurons of the entorhinal cortex, and terminate in the most distal part of the dendritic tree of CA2 pyramidal neurons (Cui et al., 2013). This projection is organized topographically: medial EC afferents terminate closer to Stratum radiatum, while lateral EC afferents do so further distally, closer to the hippocampal fissure. Whether there is a more complex topography from different rodent entorhinal cortex subfields is not known. No return projections from CA2 to the EC have been described using tract tracing methods (Cui et al., 2013), and therefore, only CA1 and subiculum project to the deep layers of the entorhinal cortex. However, in mice and rats this projection, foreseen by (Lorente de Nó, 1934), has been shown using genetically targeted rabies virus tracing (Rowland & Moser, 2013) and this calls for further research.

3.4 | Hypothalamic connections: Nonhuman primates

In nonhuman primates, the supramammillary nucleus of the posterior hypothalamus, an area dorsal to the mammillary nuclei, provides direct, specific afferents to CA2 (Veazey et al., 1982a, 1982b). In this study, deposits of anterograde neuronal tracer in the supramammillary area, labeled specifically Stratum oriens, Stratum pyramidale and the deep half of Stratum radiatum. The projection did not reach CA3 or the region of mossy fibers of CA3. However, their Figure 6 shows light labeling in a small area corresponding to Stratum lucidum at the most distal the portion of CA3, bordering CA2. Thus, the macaque monkey may also have a supramammillary projection to CA2 which overlaps with CA3. Interestingly, no projection seems to

reach the *Stratum lacunosum-moleculare*, and therefore, both projections to CA2, EC and supramammillary nucleus are segregated one from the other by their different layer termination. The distribution of the labeling extends throughout the entire longitudinal axis of CA2, and, to the contralateral CA2, albeit with lighter intensity. Furthermore, it was also suggested that caudal levels of CA2 (septal in the rodent) received a heavier projection from the supramammillary region (Veazey et al., 1982a, 1982b). Whether these findings point to a differential projection along the longitudinal axis of the hippocampus is still unknown.

In the nonhuman primate CA2 shows immunoreactivity to calcitonin and substance P which originate in the supramammillary nucleus of the hypothalamus and reach both the DG and the pyramidal layer of CA2 via fornix (Nitsch & Leranth, 1993, 1994; Seress & Leranth, 1996). Besides, neurons of the supramammillary nucleus colocalize calcitonin and substance P but they do not show GABA-positivity. Further investigations show that substance P fibers form asymmetric synapses with dendritic shafts of CA2 neurons (Nitsch & Leranth, 1994). The functional significance of this projection is barely known, other than its implication in theta activity (Berger et al., 2001).

3.5 | Hypothalamic connections: Rodents

Like in monkeys, the rodents' hippocampal field CA2 receives afferents from the posterior part of the hypothalamus. There is a prominent projection from the supramammillary nucleus. But in addition to the monkeys' hypothalamic input, another source of afferents comes from the tuberomammillary nucleus, more ventrally situated in the hypothalamus and closer the infundibulum.

Afferents to CA2 from the supramammillary nucleus terminate in the principal cell layer (Magloczky et al., 1994). This projection is restricted to CA2 and the DG, but avoids CA3 and CA1. These pathways seem to have separate functions. While the hypothalamic-DG projections is implicated in memory processing, the hypothalamic projection to CA2 appears to be related to social interactions (Chen et al., 2020). Projecting neurons from the supramammillary nucleus to CA2 show substance P immunoreactivity, and they also present calcitonin immunoreactivity.

Compared with primates, CA2 in rodents receives a minor innervation from the supramammillary nucleus (Haglund et al., 1984). In contrast the supramammillary projections to CA2 in humans and nonhuman primates are much denser than in rodents (see below). However, another source of input from the hypothalamus is vasopressin fibers from the supraoptic and paraventricular nuclei, where the subfield CA2 shows the highest immunoreactivity of all hippocampal subfields (Cui et al., 2013; Zhang & Hernandez, 2013).

3.6 | Nonhuman primates: other connectional sources

Information about CA2 connectivity in the nonhuman primate is very scarce. Cholinergic input to CA2 is among the most significant findings.

The origin of the cholinergic input to CA2, as well as for the rest of the hippocampus, is the medial septal complex and the nucleus of the diagonal band of Broca (Amaral & Cowan, 1980). One of the markers of cholinergic activity is Acetylcholinesterase (AChE), which has been extensively studied in the medial temporal region (Bakst & Amaral, 1984; Mesulam et al., 1984). However, AChE activity is not always indicative of cholinergic activity, and more specific markers such as cholineacetyl transferase (ChAT) uncover more reliably presence of AChE-positive neurons.

The distribution of acetylcholine transferase (ChAT) in the monkey HF has been extensively described by Alonso and Amaral (1995). ChAT activity has been reported along the whole rostrocaudal axis of the hippocampus. The highest density of ChAT is found at the level of the rostral part of the hippocampal body. CA2 has heavier ChAT immunoreactivity in *Stratum oriens* that stops at the boundary with the *Stratum pyramidale*. CA2 *Stratum radiatum* contains numerous ChAT positive fibers, which increased towards the *Stratum lacunosum-moleculare*, with denser staining close to the hippocampal fissure (see figure 3 in Alonso and Amaral, 1995). The transverse axis of CA2 shows a decreasing gradient in ChAT activity from CA3 towards CA1. Similar distribution of ChAT in other nonhuman primates have been reported.

Like AChE, other inputs to CA2 in nonhuman primates are not restricted to this hippocampal area but are extensive to other parts of the HF (Amaral & Cowan, 1980; Insausti et al., 1987b). Afferents include different monoaminergic groups like dopamine from the ventral tegmental area; noradrenalin from the *Locus coeruleus* and serotonin from the dorsal raphe nucleus. However, the topographic distribution of these projections and their specific laminar termination in nonhuman primates calls for further research.

3.7 | Rodents: Other connectional sources

Cholinergic afferents from the basal forebrain, bilateral medial septal nuclei together with both, the vertical and horizontal limbs of the diagonal band of Broca to CA2 have been described in rodents (Cui et al., 2013; Middleton & McHugh, 2020; Vertes & McKenna, 2000). The distribution of ChAT fibers in CA2 in rodents is slightly different from that in the macaque. The highest density of positively labeled fibers in the *Stratum lacunosum-moleculare* of the macaque are highest, while they are lowest in the rat CA2 (Houser et al., 1983).

3.8 | Ancillary inputs in rodents

Neurons in the supramammillary nucleus that project to CA2 are immunopositive for Substance P, and they also present calcitonin immunoreactivity. The latter distributes more broadly in the hippocampus, beyond CA2.

The subfield CA2 receives vasopressin fibers from the supraoptic and paraventricular nuclei of the hypothalamus. In fact, from all hippocampal subfields, CA2 together with the DG show the highest density of immunoreactivity for vasopressin (Cui et al., 2013; Zhang & Hernandez, 2013).

Brainstem inputs. One of the few studies specific to CA2 shows projections arising in the central superior and dorsal raphe nucleus (Moore & Halaris, 1975). In contrast, minor projections originate in the *locus coeruleus* or ventral tegmental area (Cui et al., 2013). This finding is consistent with the innervation from brainstem nuclei of other species (Amaral, 2023).

No direct connections of CA2 with the neocortex are known to exist.

4 | HUMAN STUDIES OF CA2

In humans, only a handful of reports deal with CA2 from a structural and connective point of view. This information is indirectly inferred from immunohistochemical studies. However, a critical starting point to understand the anatomical (including neurochemical) and functional organization of CA2 is the issue of how to define CA2 boundaries with CA3 and CA1. These boundaries are, so far, based on morphological features, although they may vary with the advance of new data from more recent techniques, such as molecular neuroanatomy or functional neuroimaging.

A 3D reconstruction of the HF, shows that CA2 can be found along the whole rostrocaudal axis of the hippocampus, an important structural finding (Figure 4). Data on the morphology of field CA2 in humans is advanced here from a larger study of the longitudinal extension of CA2 applicable to neuroimaging. In particular, high resolution neuroimaging combined with histological delimitation of CA2 is particularly useful. Data of this kind is very relevant when considering the atrophy or shrinkage of the hippocampus in neurodegenerative diseases and other neurological ailments. Closely related to anatomical changes in the hippocampus is cell number reduction in neurodegenerative diseases; the importance of the quantification has been demonstrated by unbiased stereological techniques; values of the number of neurons will be provided as specifically as possible for CA2.

A difference between experimental or descriptive studies in animal species or humans resides in the processing of brain tissue for histological verification of hippocampal fields. While most experimental studies use relatively thick sections (30–50 μm), pathology studies use commonly paraffin sections much thinner (5–7 μm). The resulting appearance of both approaches is very different, what poses some difficulties for the delimitation of CA2 from the neighboring hippocampal fields, and therefore, in the identification and quantification of pathology. We offer a guide for the identification and delimitation of CA2 in paraffin sections based in a systematic analysis of the whole extent of CA2 in Nissl stained 50 μm thick sections.

4.1 | Human CA2 appearance in Nissl-stained material

The human hippocampal CA2 field presents similarities and differences with other mammals. Common features include the classical definition of CA2, that is, the absence of mossy fiber projection, which is highlighted by the absence of *Stratum lucidum* in CA2. A second

common feature is a high cell packing density in the principal (pyramidal) layer of CA2, which contrast with the adjacent CA3 and CA1 (Figures 4 and 5). Those two characteristics are valid in general terms across species, but at some levels of the hippocampal longitudinal axis CA2 has some special features. However, there is no detailed comparative studies of the anatomy of CA2.

As it is illustrated in Figures 4 and 5, CA2 stands out as a denser, closely packed group of darkly stained neurons in Nissl-stained preparations. In fact, CA2 reaches the maximal cell packing density of all the HF subfields. In a proximal direction (towards DG) the criterion to guide the identification of the boundary of CA2 with CA3 is the loss of a homogeneous pyramidal cell layer in CA2, that shows a neat organization in rows of neurons 10–12 cells thick in CA3. In contrast with CA3, the appearance of CA2 neurons do not display such a neat organization in rows of neurons; towards CA1, pyramidal cells appear in an even more heterogeneous fashion (Figure 5).

The lateral boundary of CA2 can be oblique (Figures 1 and 5a, b) with CA2 neurons overlying over CA1 neurons. One of the most noticeable feature, already described by Ramon y Cajal (1904), and common to all mammals is the smaller size of pyramidal neurons in CA1, and the broadening of the thickness of the *Stratum pyramidale*, which can reach 15–25 neurons thick. Those distinguishing features, are also helpful landmarks for placing the boundary between CA2 and CA3.

The boundary between CA3 and CA2 is not perpendicular to the surface (Figure 5c, d), but again, it forms a line that skews at the boundary with CA3 neurons, which lie on top of CA3 neurons (Ohm et al., 1992). This arrangement can be also noticed in Timm stained or acetylcholinesterase preparations (Lim, Blume, et al., 1997; Lim, Mufson, et al., 1997; Ohm et al., 1992). Calbindin immunohistochemical stain of human hippocampus also shows this skewed boundary (Seress et al., 1993).

Cell body-stain Nissl stain of CA2 or any other cell body staining method, shows a somewhat unclear boundary between CA3 and CA2. It is even considered “arbitrary” based solely on Nissl-stained preparations (Lauer & Senitz, 2006). However, we show that in histologically well stained sections, the placement of consistent boundaries between both, CA3 and CA1 is possible and reliable (Figure 5). Under careful examination, it becomes evident that the distal portion of CA3 extends for a short distance under CA2 neurons (i.e., figure 1 in Ohm et al., 1992). Likewise, the boundary between CA2 and CA1 is difficult to establish, because CA2 neurons overlap with the proximal part of CA1, where a thinner pyramidal cell layer of CA2 can underlie CA1, which starts to increase its thickness. The boundary is not linear but there is always a mix of pyramidal neurons big and small. This organization is also observed in nonhuman primates, where neurons of CA3 overlap CA2, a morphological feature shown, i.e., in figure 17 of Rosene and van Hoesen (1987).

While neuron size is smaller in CA1, the size of neurons is similar in CA3 and CA2 fields. Neurons in these latter fields reach around 4–6 neurons thick in coronal sections. The cell bodies bordering *Stratum radiatum* are denser in terms of packing density, and they split in two or three rows towards *Stratum oriens* (Braak, 1980). Braak also noticed this feature of CA2 and indicated a “superficial and a profound lamina”, each of several rows of neurons, contain high pigment density, what provides a relatively easy delimitation. Notwithstanding, the

pigmentoarchitectonic method used by (Braak, 1980) requires very thick sections (up to 500 μm in thickness), what makes easier the visualization of layers. On the other hand, Duvernoy and Risold (2005) points the high vascularization of hippocampal subfield CA2, and attributes a possible resistance in vascular or hypoxic damage.

4.2 | Structural studies of human CA2

Neuropathological and fMRI studies report results for CA3/CA2 together, however Golgi studies in humans provide a strong morphological argument in favor of the separation of CA3 from CA2 as distinct fields. The main distinguishing feature is the presence of thorny excrescences on dendrites of CA3 neurons characteristic of the mossy fiber terminals. This pathway originates in the granule cells of the DG and is directed towards CA3 in a variety of species, as well as in humans. The Golgi silver impregnation method shows the lack of these excrescences in CA2 neurons (Lauer & Senitz, 2006), and this can be used as a guide to place the boundary between CA3 and CA2.

The classical Timm's staining method for heavy metals, specifically for zinc, highlights the mossy fiber pathway in the human CA3. The boundary between CA3 and CA2 is clearly recognizable by the characteristic black reaction of the zinc stain, which stops sharply at the CA3-CA2 border (Ohm et al., 1992).

The mossy fiber projection to CA3 has been demonstrated by tracing studies in postmortem human brain hippocampus (Lim, Blume, et al., 1997; Lim, Mufson, et al., 1997; Ohm et al., 1992). In the study of Lim, Blume, et al. (1997), the mossy fiber projection to CA3 is traced using lipophilic diffusion of carbocyanins (DiI) or biocytin. Deposits of this neuronal tracer in the DG granule cell layer of surgically excised hippocampus from patients show a sharp boundary between the end of the mossy fiber projection in CA3, excluding CA2. However, this boundary is not radially oriented, that is, parallel to the main dendrites of the pyramidal cells, but displays an oblique orientation, also observed in dynorphin immunoreactivity (Houser et al., 1990). There is a correspondence of the labeled mossy fiber projection with immunohistochemically stained for calbindin (a well-known marker for mossy fibers) in adjacent sections. This supports the extent of the projection and its boundary with CA2. This kind of studies are very difficult to replicate, and it is possible that the use of extended palette of cell-type specific markers might offer new insights (Menéndez de la Prida and Insausti, unpublished observations). This could possibly open the field to revise the traditional concepts of CA2 definition and its relationship with the mossy fiber terminal area.

4.3 | Human CA2 connections

As described previously in nonhuman primates, the human CA2 presents a few calretinin immunoreactive neurons at the distal end of *Stratum radiatum* and *Stratum lacunosum-moleculare*. In addition, dense bundles of immunoreactive puncta among pyramidal cells are present in CA2, which are larger and more heavily stained relative to

other hippocampal regions (Nitsch & Ohm, 1995). Although there is no similar tract tracing data in humans, this organization is reminiscent of the hypothalamo-hippocampal projection in primates.

The similitude of this projection between human and nonhuman primates may start during prenatal development. Berger and collaborators (Berger et al., 2001) report CA2 neurons at middle stages of gestation in human fetuses (around 20 gestational weeks). At this age, calretinin immunoreactivity is hardly present, but substance P immunoreactivity innervates CA3 and CA2. By the time of birth, the calretinin and substance P pattern of innervation resembles that of the adult. The fetal monkey supramammillary neurons express both calretinin and substance P immunoreactivity, although these do not colocalize GABA, GAD-65, or GAD-67 (Berger et al., 2001). Comparatively the supramammillary-hippocampal projection seems to develop earlier in humans than in nonhuman primates. In the latter, calretinin and substance P are detectable at 109 days out of 156 gestational days (about two-thirds of the total gestation period for macaques). This robust projection from the supramammillary nucleus to CA2 in humans and nonhuman primates stands in contrast to the rat hippocampal system, where CA2 receives minor innervation from the supramammillary nucleus. Although functionally this projection has been related to the maturation of brain theta rhythm, it still needs verification in humans (Berger et al., 2001).

4.4 | Combination of cyto-and Receptoarchitectonics

A different approach is provided by the analysis of the distribution of receptors in the human hippocampus reported by (Palomero-Gallagher et al., 2020), which, at the same time that localizes and determines quantitatively the presence of 15 neurotransmitter receptors, identifies boundaries of CA2 with other hippocampal fields. In this study, the extent of CA2 ranges from section #4201 to #294. Considering sections at 20 μm the total length of the human CA2 field is 25,200 μm , or 2.52 cm (Palomero-Gallagher et al., 2020). Likewise, the volume calculated was an average of $183 \pm 29 \text{ mm}^3$, with no significant differences between left or right hemispheres, or gender, although slightly larger CA2 volume in females was noted ($200 \pm 24 \text{ mm}^3$ in females, versus $167 \pm 26 \text{ mm}^3$ in males). Interestingly, the receptor architecture of CA2 differs in density from that of CA3 for GABA_A, GABA_B, M₁, M₃, 5-HT_{1A}, and GABA_A/BZ binding sites. Obviously, and besides other characteristics pointed out in this review, CA3 and CA2 are anatomically and functionally different fields, a concept not present in the neuroanatomy of the hippocampal formation until the decade of 1980 (Amaral & Cowan, 1980; Palomero-Gallagher et al., 2020).

4.5 | Quantitative anatomy of CA2 in the human hippocampus

The quantification of brain neurons and cells in general has attracted much attention. Earlier publications relied on the number of neurons in

a defined region (density of neurons), and led to widely variable results among studies, because this methodology was biased. The introduction and popularization of unbiased stereological techniques in the last 30 years prompted a great number of more reliable studies. The HF and its different components has been a region of interest for stereological studies, although specific data about field CA2 is, to a certain extent, disappointing. First, because the scarcity of studies and second, the difficulty in placing reliable boundaries between CA3 and CA2 in the commonly used Nissl-stained preparations in stereological studies. Most, if not all publications lump together CA2 and CA3 (Chen et al., 2020; Rogers Flattery et al., 2020b; Simic et al., 1997; West & Gundersen, 1990), and therefore, no conclusion can be drawn from these studies on CA2 neuronal number. As an approximation, (Simic et al., 1997) estimates 2.7×10^6 neurons in CA3 and CA2 together. Similar neuronal count (2.7×10^6) was obtained by West & Gundersen (1990), and replicated in a posterior study by (West, 1993) yielding a value of 2.82×10^6 neurons in both fields. A recent and independent study by (Chen et al., 2020) gave a somewhat lower value of 2.3×10^6 neurons. Moreover, the number of glial cells was found to be 6.33×10^6 , about three times the number of neurons.

Interestingly, the number of neurons is stable in Alzheimer's disease cases (2.4×10^6) relative to controls (2.3×10^6) (Simic et al., 1997), while Walker et al. (2021) report a greater loss of CA2 cells compared with CA1 in a semi-quantitative study of primary aged-related tauopathy (see below). These types of studies are the basis for the establishment of the normal status versus different neurological conditions, in particular neurodegenerative and psychiatric diseases (Malchow et al., 2014), and reinforce the need for more specific details about the HF normal neuronal and glial population across lifespan.

Size measurements, without being specifically germane to stereological studies on the number of neurons, and their possible variation in experimental conditions is of unquestionable interest in general and in particular for the CA2 field. The comparison of rat CA2 and CA1, show that CA2 neurons are comparable in size to CA3 neurons, about 30 μm in diameter, and about $700\mu\text{m}^2$ extent. In contrast, the size of CA1 neurons is 15 μm in diameter, and about $193\mu\text{m}^2$ in area (Amaral, 2023). This difference in size is also an important criterion useful for the localization of CA2 subfield boundaries.

Stereological estimations in nonhuman primate species yield a lower number of neurons in CA3-CA2 hippocampal fields relative to humans. Studies in the chimpanzee result in a total number of 0.98×10^6 (Rogers Flattery et al., 2020a) and in the rhesus monkey this value drops to 0.6×10^6 (Keuker et al., 2003).

Similarly, the interest in determining the number of neurons and glial cells in rodents derives from the experimental models of diseases, especially in genetically modified animals.

5 | TOPOGRAPHY OF HIPPOCAMPAL SUBFIELD CA2

From a gross anatomical point of view, the hippocampus is a structure made up of fields that take different appearance along its longitudinal

axis. The hippocampus starts rostrally and progresses in a caudal direction in the form of increasing number of layers that are added progressively. Therefore, hippocampal fields change their morphology and extent along the rostrocaudal axis. For instance, in a series of coronal sections, the first layer identifiable is the alveus, followed by the pyramidal layer of the Subiculum, CA1, and so on and so forth. Therefore, the field CA2 is not present from the very rostral part of the hippocampus, but arises at midlevel of the hippocampal head, and once CA3 is well formed. For this reason, and in order to interpret correctly the hippocampal fields in neuroimaging studies, we describe the appearance of CA2 along the rostrocaudal axis of the hippocampus. We studied this in a number of human cases systematically sectioned from rostral to caudal and CA1/CA2/CA3 were annotated every half a millimeter (Yushkevich et al., 2021). Moreover, we labeled other landmarks present in the medial temporal lobe (MTL) for orientation of hippocampal structures and as a reference to provide topographical relationships with CA2.

Figure 3 shows one example of a 3D reconstruction after detailed cytoarchitectonic analysis of one complete MTL and HF annotation. The beginning of CA2 in the hippocampal head and its extension as far as the caudal tip of the hippocampal tail can be appreciated. The irregularities in the boundaries with both CA3 and CA1 reflect smaller variations in the transverse extent of CA2, or variations in the interpretation of the boundaries.

We describe the changes in appearance of CA2 in a series of coronal sections in a typical control case (Figures 4 and 5, a 74 years old male) with 2 h of postmortem interval, and perfused with fixatives through both carotids (Insausti et al., 2023). The series of the hippocampus shown in Figure 4 starts at the first histological section where the Subiculum can be found, and continues caudally as far as the last section with CA2.

CA2 starts at some distance (13 mm) from the first section where the Subiculum is visible, approximately at midlevel of the amygdaloid complex. The hippocampal subfields in the series of coronal sections appear progressively, where the DG is particularly noticeable. The field CA3 starts about 2 mm just after the commencement of DG. In contrast with the detailed report of (Ding & Van Hoesen, 2015), we do not see CA2 subfield rostral to CA3 (Figure 4). We locate CA2 subfield shortly after the CA3 commencement and always interposed between CA3 and CA1. The subfield CA2 is present 5.5 mm caudal to the start of DG. At this very rostral level, the appearance of CA2 resembles closely to the architectonics of the CA3 subfield, and therefore, distinguishing both fields can be difficult. It is interesting to note that the rounded structure of the hippocampal head produces sections that appear tangentially cut. As a consequence, CA2 pyramidal cell layer appears to be thicker (more neurons in a single plane of section), relative to more caudal levels. As in can be appreciated in Figures 4 and 5 (a, b). The neurons still do not display the characteristic dark appearance of CA2 neurons seen at more caudal levels along the longitudinal axis of the hippocampus. However, CA2 can be separated from CA3 by the cell packing and high density of neurons. This point is coincident with the split of the DG granule cell layer into two hippocampal specular images of the DG approximately at midlevel of the hippocampal head (uncus). The lateral DG will eventually be

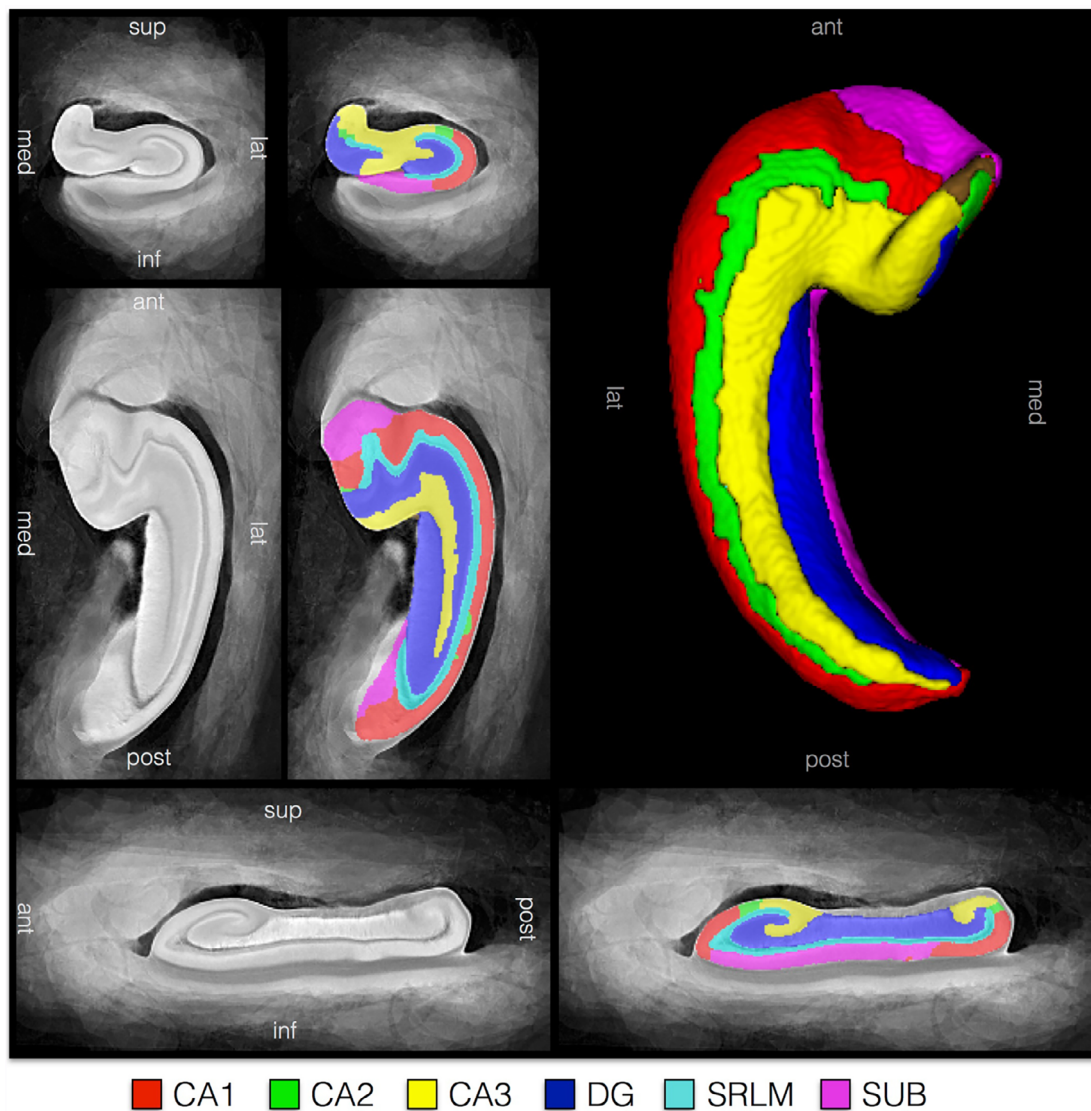


FIGURE 3 3D MRI reconstruction of the human hippocampus along the longitudinal axis serially sectioned at 50 μm from rostral to caudal, Nissl-stained with thionin and annotated following the criterion in the text. Annotations were translated onto 9.4 T ex-vivo MRI by ITK-Snap software, and reconstructed as in Yushkevich et al., 2021 (Yushkevich et al., 2021). Coronal, axial and sagittal cross sections are also shown. Green color corresponds to CA2, which can be seen starting caudal to CA3, and extending up to the hippocampal tail.

continuous with the body of the hippocampus, while the medial extension, more irregular in shape, is continuous with the hippocampal fields of the *Gyrus uncinatus*. The uncus ends as *Gyrus intralimbicus*, made up of field CA3, 1.5 mm behind the start of CA2. The uncus extension of CA2 is very short, (about 1.5 mm). The end of the hippocampal head, marked by the *Gyrus intralimbicus*, cedes the way to the beginning of the hippocampal body.

A typical cross section of the hippocampus is shown in Figure 4e,f. At this mid-level, the boundaries of CA2 can be clearly distinguished: CA3 subfield is several rows of cells thick (about 12) relative to CA2 (around 8). CA2 has a cellular appearance is much more compact, the space between neurons much narrower, and the constituting neurons look more disorganized and heterogeneous and the principal, pyramidal cell layer does not present apparent subdivisions.

Another distinguishing feature of CA3/CA2 boundary is the presence of *Stratum lucidum*, the site of the mossy fiber terminals. The *Stratum lucidum* appears with lower density of glial and other cells, especially near the pyramidal cell layer. Although the Nissl-stain is not by itself a marker of the mossy fiber projection, nonetheless, it offers a simple method to assess approximately the extent this projection.

The boundary of CA2 with CA1 is better distinguishable when CA2 pyramidal cell layer decreases in thickness (up to 4–6 neurons thick), and overlaps for a short distance with CA1 (Figure 5a,b). In contrast, the thickness of CA1 (10–12 rows of neurons), as well as the smaller neuronal size characteristic of CA1, makes the boundary apparent. The transition CA2–CA1 is not sharp, but neurons of both subfields intermingle, and the farthest CA2 neurons lie on top of the most proximal portions of CA1.

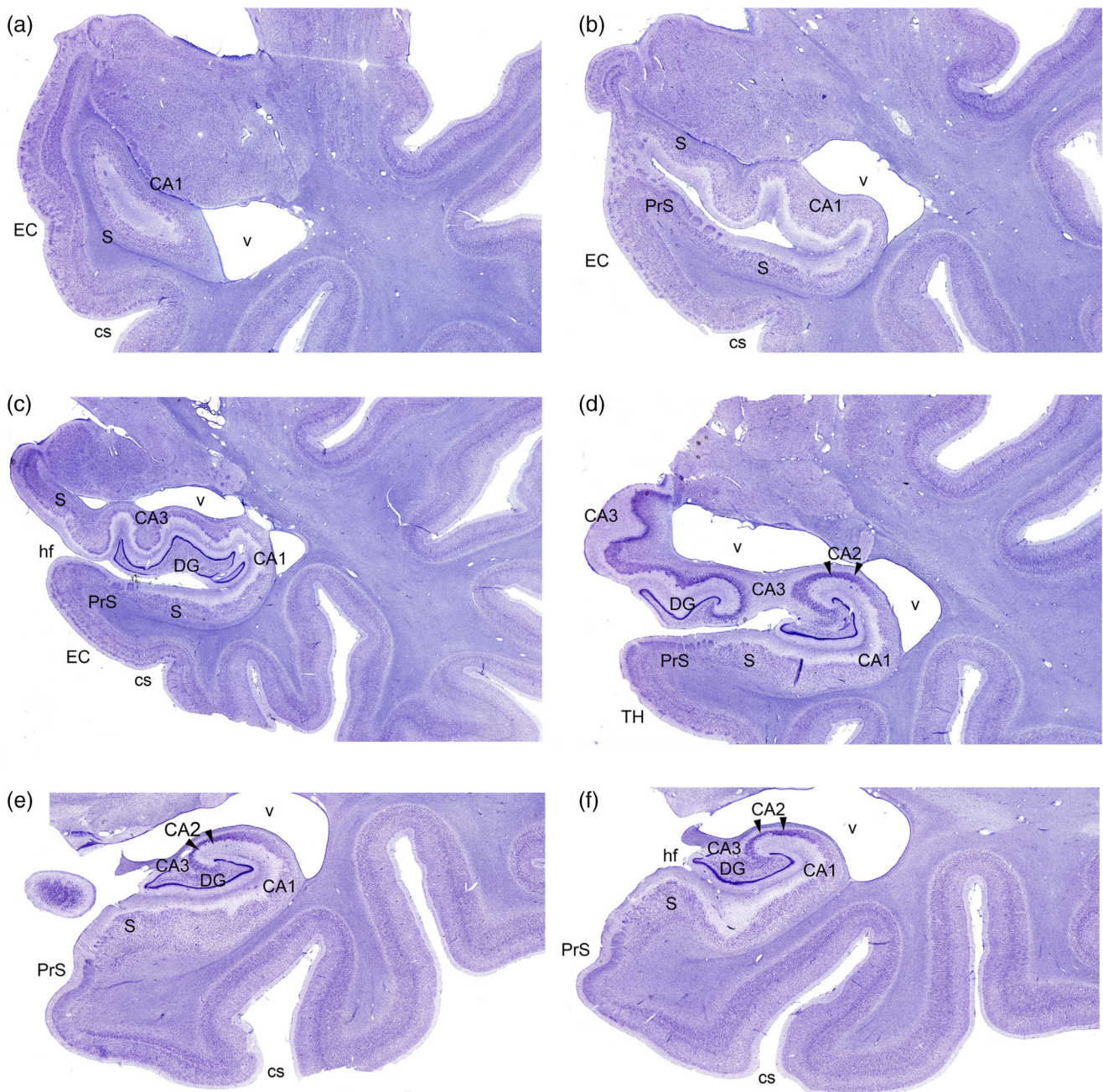


FIGURE 4 The field CA2 of the human hippocampus is shown in low-power photomicrographs of a control case (HNL46-19, male, 74 years old, and 2 h of postmortem interval). The illustration shows the location and cytoarchitecture of field CA2 of the hippocampus in Nissl-stained coronal sections through the hippocampus from rostral to caudal, spanning from the rostral hippocampal head (A) to the hippocampal tail (L). The plane of section is perpendicular to the ac-pc line. (a) Rostral head of the hippocampus. (b) Middle head of the hippocampus. (c) Mid-caudal head (note the open hippocampal fissure). (d) Caudal head at the level of the Giacomini band. (e) Caudal end of the hippocampal head at the level of the *Gyrus intralimbicus*. (f) Rostral part of the hippocampal body. (g) Mid portion of the hippocampal body. (h) Mid-caudal part of the hippocampal body. (i) Caudal part of the body. (j) Rostral part of the hippocampal tail. (k) Midportion of the hippocampal tail. (l) Caudal portion of the hippocampal tail. Note that subiculum, CA1 and CA3 lie rostral to the start of CA2 (D). From that point on, CA2 extent corresponds to the stretch between arrowheads. Little variation takes place across rostrocaudal levels, both in location and extent. CA1: CA1 subfield of the hippocampus. CA2: CA2 subfield of the hippocampus; CA3: CA3 subfield of the hippocampus; cs: collateral sulcus; DG: dentate gyrus; EC: entorhinal cortex; hf: hippocampal fissure; PrS: Presubiculum; S: Subiculum; v: lateral ventricle (temporal horn). Scale bar corresponds to 2 mm.

About 10 mm behind this point (most of the posterior part of the hippocampal body), the overall look of CA2 is homogenous with little differences (Figures 4 and 5). However, CA2 blends both at its proximal

and distal ends with CA3 and CA1, respectively, in such a way that neurons intermingle at the boundaries. The clear *Stratum radiatum* decreases in size, and although still visible, it looks continuous with

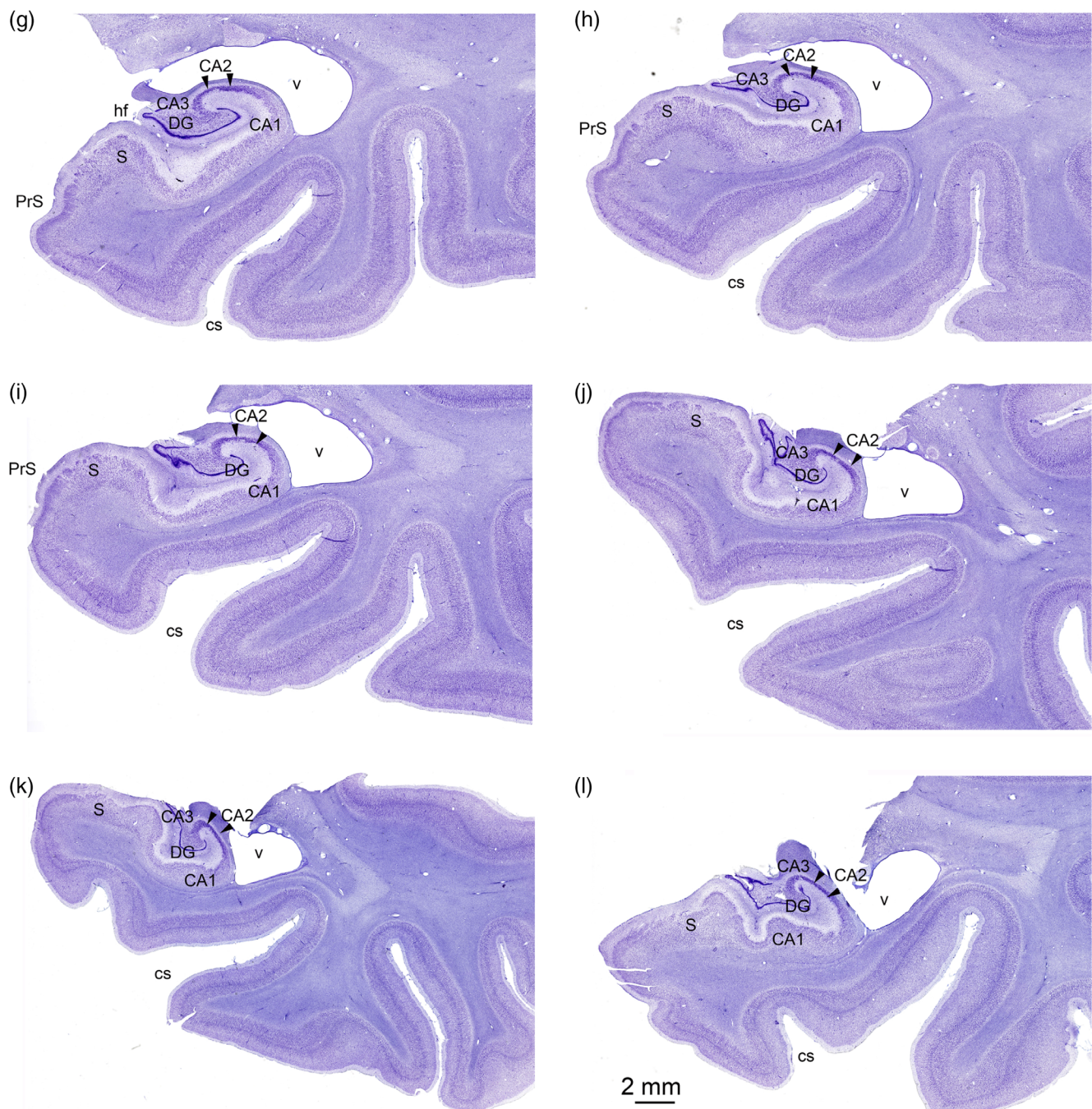


FIGURE 4 (Continued)

Stratum radiatum in CA1. In contrast, the clear band of the mossy fiber keeps its location clearly defined, and still is a useful overall landmark.

The hippocampus caudal end, the tail, about 5 mm caudal to the previous level coincides with an inclination in a dorsal direction of the hippocampal axis to eventually reach the hippocampal commissure under the splenium of the corpus callosum. The DG, along with the remainder of the hippocampal fields, change the usual topographical organization of the hippocampal body, due to the increasingly verticalization of the whole hippocampus. In consequence, hippocampal sections appear progressively more tangentially sectioned, so hippocampal subfields look as if “stretched” (Figures 4*l* and 5*f*).

5.1 | CA2 delimitation in thin, 5–10 μ m (paraffin) sections

Neuropathological examinations use much thinner preparations (around 5–10 μ m), compared with other basic neuroscience studies, which range 30–50 μ m thick. Besides, the most common stain is Hematoxylin-Eosin (HE), which stain neatly cell bodies and nuclei, but that makes difficult the separation among fields (Farrell et al., 2022). Usually, pathological studies of the hippocampus are limited to a single level, generally to the hippocampal body. This has the advantage that all layers shown in Figure 1 are easily identifiable. The criteria

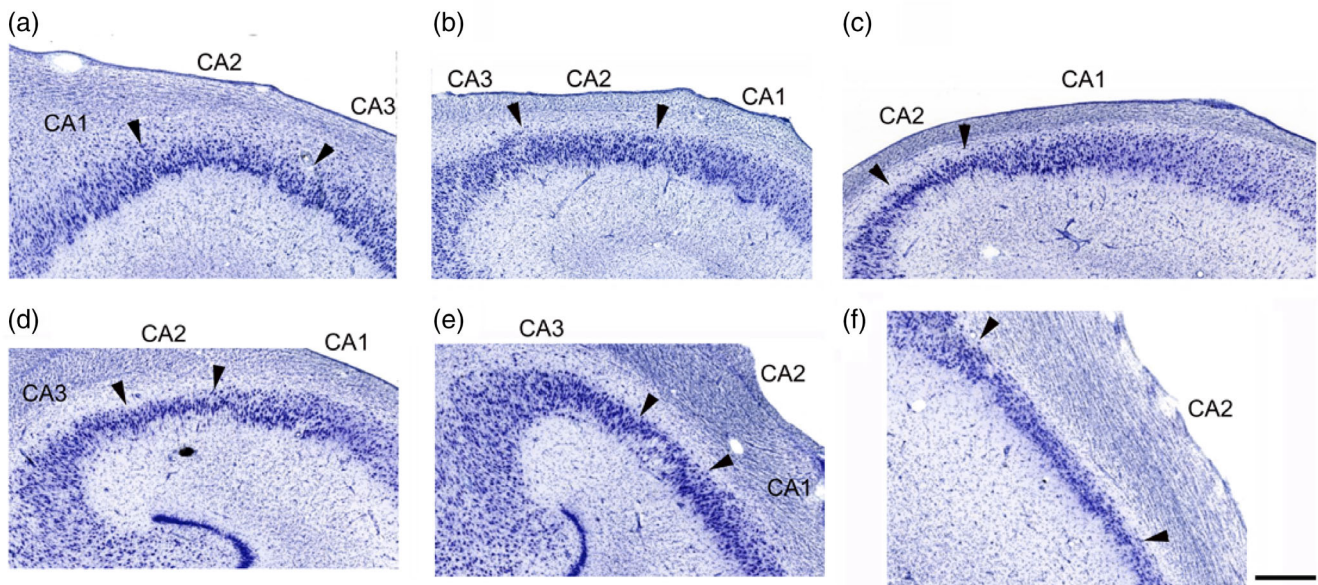


FIGURE 5 Photomicrograph of field CA2 from human control brain (HNL46-19, male, 74 years old with 2 h of postmortem interval) at different rostrocaudal levels. (a) Field CA2 at the level of the uncus (uncal CA2, same level as in Figure 2d). (b) CA2 at rostral level of the hippocampus body (same level as in Figure 2a). (c) Field CA2 at mid-level of the hippocampus body, just caudal to the *Gyrus intralimbicus* (end of uncal CA3). (d) Field CA2 at the caudal part of the hippocampus body. (e) Field CA2 at the commencement of the hippocampus tail. (f) Field CA2 at the level of the caudal end of the hippocampal tail. The variation in shape, extent and cytoarchitecture of area CA2 is minimal along the rostrocaudal axis of the HF, but the boundaries with adjoining regions CA1 and CA3 are specially stretched in panel F because of the skewness at the end of the hippocampus. See text for details. Scale bar corresponds to 250 μm .

stated above (neuron size as CA3, smaller size of CA1 neurons, higher packing density, heterogeneous and disorganized appearance of the neurons) can also be appreciated in regular HE paraffin sections. However, immunohistochemical staining (i.e., Substance P in particular) add assurance to the delimitation of the subfield CA2 (Farrell et al., 2022).

5.2 | Subfield CA2 in the longitudinal extent of the hippocampus

We measured the length of CA2 in 23 cases (10 females, 43% with a mean age of 73.17 ± 11.18). On average, the rostrocaudal length of the hippocampus field CA2 was 28.97 ± 4.45 mm (Figure 6). No sex difference was found (Univariate ANOVA, $F_{21} = 0.049$, $p > .828$). Likewise, no association of age with the longitudinal size of CA2 was found (Spearman partial correlation $r = -0.068$, $p > .759$), having had controlled for gender.

5.3 | Rethinking CA2 boundaries of Human CA2 relative to rodent data

The criteria of (Lorente de N3, 1934) for the definition of subfield CA2 was based on Golgi material of the mouse hippocampus, which he interpreted as a distinct field that did not present mossy fibers (specific for CA3), and which was located distal (away from) to CA3.

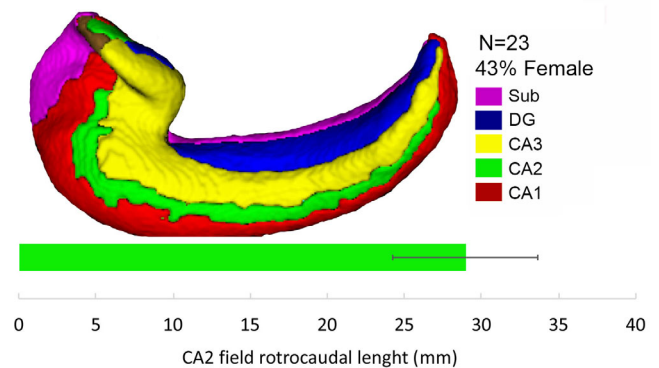


FIGURE 6 The mean length of the hippocampal subfield CA2 in millimeters is shown in the horizontal (mean \pm SD, $N = 23$, 43% females). The 3D reconstruction of the whole human hippocampus illustrates the location and rostrocaudal extent of field CA2 in the human brain. The small patch of CA2 anterior to CA3 in the uncus is an effect of the rotation of the 3D reconstruction.

However, as part of the exciting field of gene expression data in the hippocampus, which in a large extent recapitulates classical neuroanatomical studies, also shows interesting differences. The study of Lein et al., (2004, 2005) shows that CA2 subfield division of the hippocampus is somewhat larger compared with the cytoarchitectonic dimension based on Nissl-stained preparations. Specifically, CA2 is noticeable when marked for the gene PCP4 (Purkinje cell protein 4), which also marks the DG. Other genetic markers also reinforce the

notion of a wider extent for CA2 hippocampal subfield (Lee et al., 2010; Shinohara et al., 2012). However, the lack of human studies leaves open the possibility that CA2 boundaries in humans might be restated.

6 | NEUROPATHOLOGICAL STUDIES

It has been known since the XIX century that CA2 is part of what is considered a “resistant” sector of hippocampal damage, to vascular insults and epilepsy, in contrast to CA1 and proximal Subiculum (Sommer's sector which suffer great neuron loss; Zola-Morgan et al., 1986). In addition to this well-known characteristic, there are several diseases that seem to specially affect CA2.

In the following sections we would like just to offer a glimpse and illustrate the involvement of CA2 in some neuropathologies.

6.1 | Alzheimer disease

Given the lack of information on the connectivity of human CA2 field, data from pathological cases opens a window through which physiological and pathological conditions can be used to advance in the understanding the normal anatomy and abnormal cellular patterns in patients' HF.

Pathological conditions such as Alzheimer's disease (AD) and other tauopathies allow to suspect presumed projections and associated functions, as it is widely accepted that AD neuropathology extends transsynaptically following the connectivity steps largely coincident with experimental animals. For example, the study by Ding et al. (2010) shows a coexistence in layer II of neurofibrillary tangles accumulation in the entorhinal cortex, associated with tau-positive fibrillar material in CA2. The tau-positive reactivity was present in both, *Stratum lacunosum-moleculare* but extending onto the outer one-half of the of the *Stratum radiatum* of CA2. This tau-positive fibrillar material in *Stratum radiatum* was not found in either CA3 or CA1. Tracing techniques in nonhuman primates in the same study showed a projection from the EC to *Stratum radiatum* of CA2, similar to that observed in the human counterpart. Altogether, it is suggested that this projection might be specific for human and nonhuman primates. Our own examination of neuropathological material extends this finding to encompass the complete rostrocaudal extent of CA2.

As shown in Figure 7, four rostrocaudal levels in a 82-year-old female case, neuropathologically diagnosed with frontotemporal lobar dementia and transactive response DNA binding protein 43 or FTLTDP (Nelson et al., 2019). The tissue was stained for Tau protein (AT8 antibody). In this case, there were abundant neurofibrillary tangles and neuropil threads in cell bodies of CA2. The pathology extended from the uncus part of CA2 (A), in continuation with the rostral body (B), caudal part of the body (C) and tail of the hippocampus (D). The pathology increased caudally, in particular the density of neuropil threads. While the uncus and rostral body of CA2 (A, B) showed individual neurons laden with neurofibrillary tangles, in the two caudal

levels (C, D), individual neurons were obscured by the density of Tau-positive material in the neuropil. In contrast, CA3 had occasional Tau positive neurons (especially evident in C). At all levels, neurodegeneration affected *Stratum oriens*, *pyramidale* and *radiatum*, while it was lighter in density in *Stratum lacunosum-moleculare*.

In contrast, Ding et al (Ding et al., 2010) studied six cases with Alzheimer's disease, showing a coexistence of layer II neurofibrillary tangles accumulation in the EC, associated to tau-positive fibrillar material in CA2. This Tau-positive material accumulated both on the *Stratum lacunosum-moleculare* and on the superficial part of *Stratum radiatum* of CA2 (closer to *Stratum lacunosum-moleculare*), which was not found in either CA3 or CA1 (Ding et al., 2010). We interpret our lack of evidence for tau-positive immunoreactivity in *Stratum lacunosum-moleculare* as a different pattern of distribution of Tau material in FTLTDP. In this regard, selective Tau pathology in CA2 has also been reported in another form of neurodegenerative disease, Argrophilic Grain Disease, (Apostolova et al., 2015; Yokota et al., 2007), as well as in Primary Age-Related Tauopathy (PART) (Walker et al., 2021). This data calls for further research to determine detailed topographical differences in the pattern of tau-positive cells in the hippocampus.

Another common form of neurodegeneration is Parkinson's disease and the dementia form of Lewy body disease (Pang et al., 2019). Interestingly, there is a specific accumulation of pathology (α -synuclein) in CA2 (Flores-Cuadrado et al., 2016), although there is no variation in the number of neurons (Joelving et al., 2006; Villar-Conde et al., 2021).

6.2 | Schizophrenia

Changes in the hippocampus of patients with schizophrenia have been described previously (Kovelman & Scheibel, 1984). However, still much controversy exists on the role of the hippocampus in the pathogenesis of this disease (Casanova & Rothberg, 2002). Schizophrenia is a multifactorial disease (Barondes, 1998; Falkai & Moller, 2012), but some neuropathological studies mention the involvement of CA2. Nowadays, disorganization of the CA2 pyramidal cell layer is controversial and not a generalized view of the disease (Casanova & Rothberg, 2002). Likewise, the identification of neurons of smaller size relative to controls have also been reported (Arnold et al., 1995; Benes et al., 1991). More precise evaluation by stereological methods may shed light in the association of changes in CA2 in brains with this disorder (Benes et al., 1991; Heckers et al., 1991). Schizophrenia patients showed a specific 40% reduction in the number of non-pyramidal cells. In contrast, the number of pyramidal principal cells had no variation in number in any of the hippocampal CA subfields (Benes et al., 1991; Heckers et al., 1991). Overall, these results suggest that no differences exist in the number of neurons in the hippocampus, including CA3-CA2, thereby the question whether principal cell involvement in schizophrenia exists cannot be answered at this time.

More subtle effects may be of interest in the analysis of neurotransmitter density and distribution in CA2 in schizophrenia. Benes

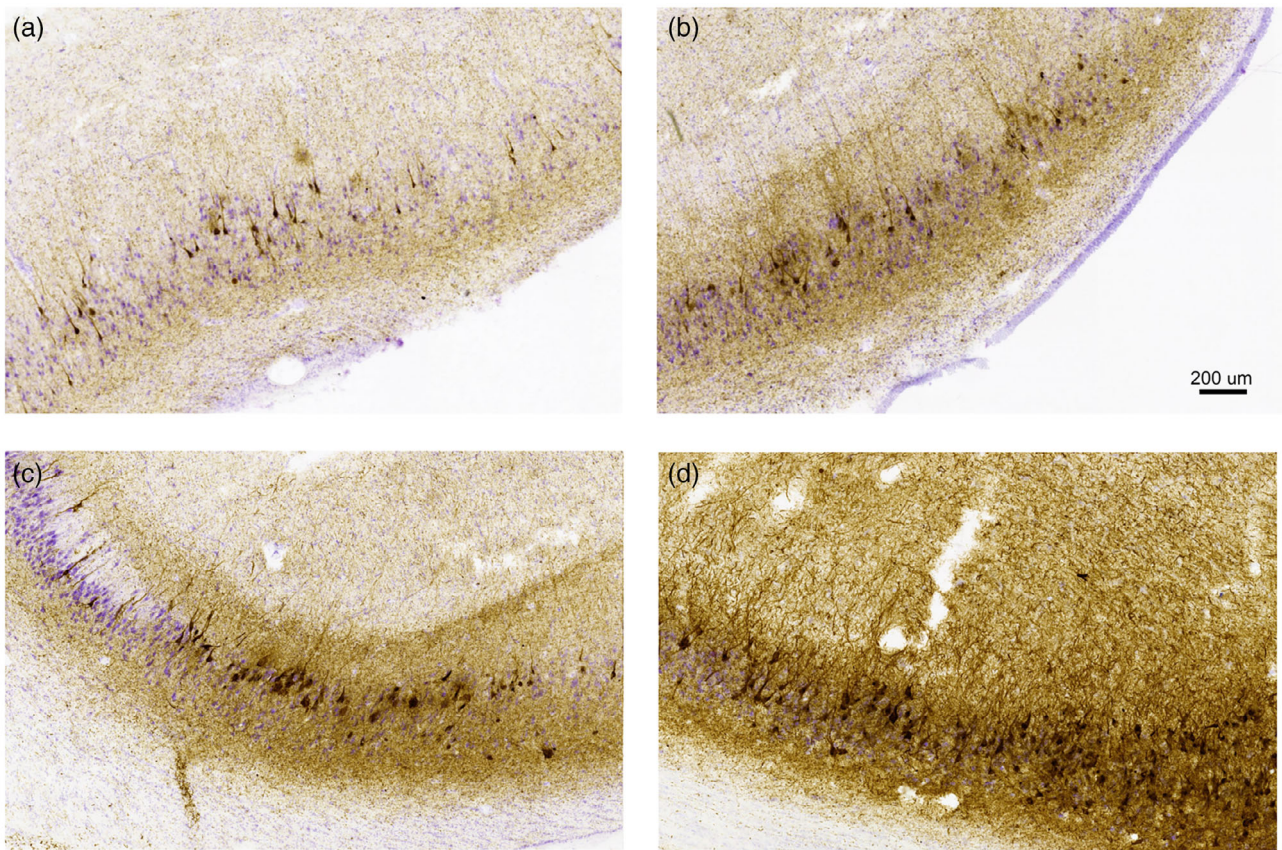


FIGURE 7 Photomicrographs of a case with frontotemporal dementia with Tau immunostaining and weakly counterstained with Nissl. (a) Neurofibrillary tangles (NFT) in uncal CA2. Note the low concentration of Tau-positive threads and punctae in the neuropil. (b) Field CA2 immunostained for Tau protein in the rostral body of the hippocampus. Note the increase in Tau-positive neuropil and some apical dendrites, as well as in Stratum radiatum, but not in Stratum lacunosum-moleculare. (c) Field CA2 at the level of the caudal part of the hippocampal body shows an increasingly heavier Tau deposits both in *Stratum oriens* and *Stratum radiatum* (proximal part) relative to both previous levels. (d) Field CA2 at the level of the hippocampal tail, where the density of the tau-positive deposit obscures any remaining neuron. CA1 is to the right-hand side, and CA3 to the left-hand side, both with comparatively lighter Tau-positive immunoreactivity and fewer labeled neurons.

et al. (2001) report a decrease of 30–35% in density of GluR_{5,6,7} immunoreactivity in *Stratum radiatum* and *Stratum lacunosum-moleculare* in schizophrenia. This reduction is more significant since GluR_{5,6,7} immunoreactivity density in apical dendrites in *Stratum radiatum* and *Stratum lacunosum-moleculare* was higher in CA2 relative to CA3 or CA1 (Benes et al., 2001). Thus, a more subtle effects of transmission in CA2 may be of importance in schizophrenia.

6.3 | Epilepsy

Epilepsy is a complex entity with multiple etiological causes and manifestations. We only refer here to epilepsy associated to the temporal lobe and hippocampus or Temporal Lobe Epilepsy (TLE) (Badawy et al., 2013). TLE is typically associated with mesial temporal sclerosis or hippocampal sclerosis (Babb & Brown, 1986). Mesial temporal sclerosis involves hippocampus, amygdala and entorhinal cortex, with neuron loss and gliosis that affects mostly subfield CA1, followed by CA3, but with little impact in CA2, which was therefore, called resistant sector (Falconer, 1974; Margerison & Corsellis, 1966). The reason

why CA2 is more resistant to mesial temporal sclerosis relative to other dentate gyrus and hippocampal fields is unclear, but data suggest CA2 pyramidal cells play major roles in the configuration of epileptogenic microcircuits (Kilias et al., 2022). Mossy fiber sprouting towards the dentate gyrus has been reported (Houser et al., 1990), where reorganization of connections extend the mossy fibers into CA2, as demonstrated by immunoreactivity to dynorphin. In human, synaptopodin-positive mossy fibers were found in CA2 and even in CA1 in close association with granule cell dispersion (Freiman et al., 2021).

In conclusion, under mesial temporal sclerosis notable reorganization of connectivity takes place, thus altering the “standard” hippocampal-cortical and possibly diencephalic set of connections.

6.4 | Further directions

This review starts to describe the anatomical appearance of the hippocampal field CA2 in humans and highlights the unknowns in terms of connectivity and function. While direct investigations on human

CA2 are not common, they provide enough basis to consider it similar to other species. Nonhuman primates, with which important morphological similarities are shared, are of notable importance mainly through the anatomical and functional connectivity between the EC, the cortex and other structures. On the other hand, nonhuman primates allow the experimental approaches presently applied to rodent species, thus making a hinge for the extrapolation of experimental data to nonhuman primates, and possibly to the human clinical setting.

In the nonhuman primate the canonical view of the flow of information through the HF connections states that layer II neurons of the EC innervate the *Stratum lacunosum-moleculare* of CA2 (in addition to CA3 and the molecular layer of the DG). In principle, this projection does not differ from that of EC-CA3. However, the termination of EC afferents in *Stratum radiatum* makes a difference with the adjacent CA3 and CA1 fields. The significance of this specific projection, the possible interaction with other inputs (i.e., the hypothalamus), and local circuits through interneurons, may be of significance in various forms of normal and abnormal behaviors, such as social memory (Chevalyere & Piskorowski, 2016). This might yet be an important implication for information flow through possibly EC-CA2 direct connections.

ACKNOWLEDGMENTS

We would like to thank Mercedes Iñiguez de Onzoño, Alicia Vela Horcajada, Esther Buendía Rosado for their technical assistance with the preparation of histological material. This study was funded by Grants UCLM 2020-GRIN-28837, and the US National Institutes of Health R01 AG056014.

DATA AVAILABILITY STATEMENT

Data is available upon request.

ORCID

Monica Muñoz-López  <https://orcid.org/0000-0002-5530-2394>

REFERENCES

- Alonso, J. R., & Amaral, D. G. (1995). Cholinergic innervation of the primate hippocampal formation. I. Distribution of choline acetyltransferase immunoreactivity in the *Macaca fascicularis* and *Macaca mulatta* monkeys. *The Journal of Comparative Neurology*, 355(2), 135–170. <https://doi.org/10.1002/cne.903550202>
- Amaral, D., & Cowan, W. (1980). Subcortical afferents to the hippocampal formation in the monkey. *The Journal of Comparative Neurology*, 189(4), 573–591. <https://doi.org/10.1002/cne.901890402>
- Amaral, D. G., Lavenex, P., & Insausti R. (2023). Hippocampal formation. In R. M. Per Andersen, D. Amaral, T. Bliss, & J. O'Keefe (Eds.), *The hippocampus book (in press)* (2nd ed.). Oxford University Press.
- Apostolova, L. G., Zarow, C., Biado, K., Hurtz, S., Boccardi, M., Somme, J., Honarpisheh, H., Blanken, A. E., Brook, J., Tung, S., Lo, D., Ng, D., Alger, J. R., Vinters, H. V., Bocchetta, M., Duvernoy, H., Jack, C. R., Jr., Frisoni, G. B., & EADC-ADNI Working Group on the Harmonized Protocol for Manual Hippocampal Segmentation. (2015). Relationship between hippocampal atrophy and neuropathology markers: A 7T MRI validation study of the EADC-ADNI Harmonized Hippocampal Segmentation Protocol. *Alzheimers Dement*, 11(2), 139–150. <https://doi.org/10.1016/j.jalz.2015.01.001>
- Arnold, S. E., Franz, B. R., Gur, R. C., Gur, R. E., Shapiro, R. M., Moberg, P. J., & Trojanowski, J. Q. (1995). Smaller neuron size in schizophrenia in hippocampal subfields that mediate cortical-hippocampal interactions. *The American Journal of Psychiatry*, 152(5), 738–748. <https://doi.org/10.1176/ajp.152.5.738>
- Babb, T. L., & Brown, W. J. (1986). Neuronal, dendritic, and vascular profiles of human temporal lobe epilepsy correlated with cellular physiology in vivo. *Advances in Neurology*, 44, 949–966.
- Badawy, R. A., Jackson, G. D., Berkovic, S. F., & Macdonell, R. A. (2013). Cortical excitability and refractory epilepsy: A three-year longitudinal transcranial magnetic stimulation study. *International Journal of Neural Systems*, 23(1), 1250030. <https://doi.org/10.1142/S012906571250030X>
- Bakst, I., & Amaral, D. G. (1984). The distribution of acetylcholinesterase in the hippocampal formation of the monkey. *The Journal of Comparative Neurology*, 225(3), 344–371. <https://doi.org/10.1002/cne.902250304>
- Barondes, S. H. (1998). Will genetics revolutionize psychiatry? *The Harvard Mental Health Letter*, 15(5), 4–6.
- Benavides-Piccione, R., Regalado-Reyes, M., Fernaud-Espinosa, I., Kastanauskaitė, A., Tapia-Gonzalez, S., Leon-Espinosa, G., Rojo, C., Insausti, R., Segev, I., & DeFelipe, J. (2020). Differential structure of hippocampal CA1 pyramidal neurons in the human and mouse. *Cerebral Cortex*, 30(2), 730–752. <https://doi.org/10.1093/cercor/bhz122>
- Benes, F. M., McSparran, J., Bird, E. D., SanGiovanni, J. P., & Vincent, S. L. (1991). Deficits in small interneurons in prefrontal and cingulate cortices of schizophrenic and schizoaffective patients. *Archives of General Psychiatry*, 48(11), 996–1001. <https://doi.org/10.1001/archpsyc.1991.01810350036005>
- Benes, F. M., Todtenkopf, M. S., & Kostoulakos, P. (2001). GluR5,6,7 subunit immunoreactivity on apical pyramidal cell dendrites in hippocampus of schizophrenics and manic depressives. *Hippocampus*, 11(5), 482–491. <https://doi.org/10.1002/hipo.1065>
- Berger, B., Esclapez, M., Alvarez, C., Meyer, G., & Catala, M. (2001). Human and monkey fetal brain development of the supramammillary-hippocampal projections: A system involved in the regulation of theta activity. *The Journal of Comparative Neurology*, 429(4), 515–529. [https://doi.org/10.1002/1096-9861\(20010122\)429:4<515::aid-cne1>3.0.co;2-2](https://doi.org/10.1002/1096-9861(20010122)429:4<515::aid-cne1>3.0.co;2-2)
- Booker, S. A., & Vida, I. (2018). Morphological diversity and connectivity of hippocampal interneurons. *Cell and Tissue Research*, 373(3), 619–641. <https://doi.org/10.1007/s00441-018-2882-2>
- Botcher, N. A., Falck, J. E., Thomson, A. M., & Mercer, A. (2014). Distribution of interneurons in the CA2 region of the rat hippocampus. *Frontiers in Neuroanatomy*, 8, 104. <https://doi.org/10.3389/fnana.2014.00104>
- Braak, E. (1980). On the structure of IIIab-pyramidal cells in the human isocortex. A Golgi and electron microscopical study with special emphasis on the proximal axon segment. *Journal für Hirnforschung*, 21(4), 437–442.
- Caruana, D. A., Alexander, G. M., & Dudek, S. M. (2012). New insights into the regulation of synaptic plasticity from an unexpected place: hippocampal area CA2. *Learning & Memory*, 19(9), 391–400. <https://doi.org/10.1101/lm.025304.111>
- Casanova, M. F., & Rothberg, B. (2002). Shape distortion of the hippocampus: A possible explanation of the pyramidal cell disarray reported in schizophrenia. *Schizophrenia Research*, 55(1–2), 19–24. [https://doi.org/10.1016/S0920-9964\(01\)00201-8](https://doi.org/10.1016/S0920-9964(01)00201-8)
- Chen, F., Bertelsen, A. B., Holm, I. E., Nyegaard, J. R., Rosenberg, R., & Dorph-Petersen, K. A. (2020). Hippocampal volume and cell number in depression, schizophrenia, and suicide subjects. *Brain Research*, 1727, 146546. <https://doi.org/10.1016/j.brainres.2019.146546>
- Chevalyere, V., & Piskorowski, R. A. (2016). Hippocampal area CA2: An overlooked but promising therapeutic target. *Trends in Molecular*

- Medicine*, 22(8), 645–655. <https://doi.org/10.1016/j.molmed.2016.06.007>
- Cui, F., Ji, J., Lv, H., Qu, D., Yu, C., Yang, Y., & Xu, Y. (2013). Immune responsiveness in a mouse model of combined adoptive immunotherapy with NK and dendritic cells. *Journal of Cancer Research and Therapeutics*, 9(Suppl), S162–S168. <https://doi.org/10.4103/0973-1482.122516>
- Ding, S. L., Haber, S. N., & Van Hoesen, G. W. (2010). Stratum radiatum of CA2 is an additional target of the perforant path in humans and monkeys. *Neuroreport*, 21(4), 245–249. <https://doi.org/10.1097/WNR.0b013e328333d690>
- Ding, S. L., & van Hoesen, G. W. (2015). Organization and detailed parcellation of human hippocampal head and body regions based on a combined analysis of cyto- and chemoarchitecture. *The Journal of Comparative Neurology*, 523(15), 2233–2253. <https://doi.org/10.1002/cne.23786>
- Duvernoy, H. M., Cat, F., & Risold, P.-Y. (2005). *The human hippocampus. functional anatomy, vascularization and serial sections with MRI*. Springer Berlin.
- Falconer, M. A. (1974). Mesial temporal (Ammon's horn) sclerosis as a common cause of epilepsy: Aetiology, treatment, and prevention. *Lancet*, 2(7883), 767–770. [https://doi.org/10.1016/s0140-6736\(74\)90956-8](https://doi.org/10.1016/s0140-6736(74)90956-8)
- Falkai, P., & Moller, H. J. (2012). Psychopathology: Genetics and the stress-vulnerability hypothesis. *European Archives of Psychiatry and Clinical Neuroscience*, 262(3), 181–182. <https://doi.org/10.1007/s00406-012-0307-x>
- Farrell, K., Iida, M. A., Cherry, J. D., Casella, A., Stein, T. D., Bieniek, K. F., Walker, J. M., Richardson, T. E., White, C. L., Alvarez, V. E., Huber, B. R., Dickson, D. W., Insausti, R., Dams-O'Connor, K., Part Working Group, AC, M. K., & Crary, J. F. (2022). Differential vulnerability of hippocampal subfields in primary age-related tauopathy and chronic traumatic encephalopathy. *Journal of Neuropathology and Experimental Neurology*, 81(10), 781–789. <https://doi.org/10.1093/jnen/nlnc066>
- Fernandez-Lamo, I., Gomez-Dominguez, D., Sanchez-Aguilera, A., Oliva, A., Morales, A. V., Valero, M., Cid, E., Berenyi, A., & de la Prida, L. M. (2019). Proximodistal organization of the CA2 hippocampal area. *Cell Reports*, 26(7), 1734–1746 e1736. <https://doi.org/10.1016/j.celrep.2019.01.060>
- Flores-Cuadrado, A., Ubeda-Bañon, I., Saiz-Sanchez, D., de la Rosa-Prieto, C., & Martinez-Marcos, A. (2016). Hippocampal α -synuclein and interneurons in Parkinson's disease: Data from human and mouse models. *Movement Disorders*, 31(7), 979–988. Portico. <https://doi.org/10.1002/mds.26586>
- Freiman, T. M., Häussler, U., Zentner, J., Doostkam, S., Beck, J., Scheiwe, C., Brandt, A., Haas, C. A., & Puhahn-Schmeiser, B. (2021). Mossy fiber sprouting into the hippocampal region CA2 in patients with temporal lobe epilepsy. *Hippocampus*, 31(6), 580–592. <https://doi.org/10.1002/hipo.23323>
- Freund, T. F., & Buzsaki, G. (1996). Interneurons of the hippocampus. *Hippocampus*, 6(4), 347–470. [https://doi.org/10.1002/\(SICI\)1098-1063\(1996\)6:4<347::AID-HIPO1>3.0.CO;2-I](https://doi.org/10.1002/(SICI)1098-1063(1996)6:4<347::AID-HIPO1>3.0.CO;2-I)
- Haglund, L., Swanson, L. W., & Kohler, C. (1984). The projection of the supramammillary nucleus to the hippocampal formation: an immunohistochemical and anterograde transport study with the lectin PHA-L in the rat. *The Journal of Comparative Neurology*, 229(2), 171–185. <https://doi.org/10.1002/cne.902290204>
- Heckers, S., Heinsen, H., Geiger, B., & Beckmann, H. (1991). Hippocampal neuron number in schizophrenia. A stereological study. *Archives of General Psychiatry*, 48(11), 1002–1008. <https://doi.org/10.1001/archpsyc.1991.01810350042006>
- Houser, C. R., Crawford, G. D., Barber, R. P., Salvaterra, P. M., & Vaughn, J. E. (1983). Organization and morphological characteristics of cholinergic neurons: an immunocytochemical study with a monoclonal antibody to choline acetyltransferase. *Brain Research*, 266(1), 97–119. [https://doi.org/10.1016/0006-8993\(83\)91312-4](https://doi.org/10.1016/0006-8993(83)91312-4)
- Houser, C. R., Miyashiro, J. E., Swartz, B. E., Walsh, G. O., Rich, J. R., & Delgado-Escueta, A. V. (1990). Altered patterns of dynorphin immunoreactivity suggest mossy fiber reorganization in human hippocampal epilepsy. *The Journal of Neuroscience*, 10(1), 267–282.
- Hunt, D. L., Linaro, D., Si, B., Romani, S., & Spruston, N. (2018). A novel pyramidal cell type promotes sharp-wave synchronization in the hippocampus. *Nature Neuroscience*, 21(7), 985–995. <https://doi.org/10.1038/s41593-018-0172-7>
- Insausti, R., & Amaral, D. G. (2008). Entorhinal cortex of the monkey: IV. Topographical and laminar organization of cortical afferents. *The Journal of Comparative Neurology*, 509(6), 608–641. <https://doi.org/10.1002/cne.21753>
- Insausti, R., & Amaral, D. G. (2012). Hippocampal formation. In J. K. Mai & G. Paxinos (Eds.), *The human nervous system* (3rd ed., pp. 896–942). Academic Press.
- Insausti, R., Amaral, D. G., & Cowan, W. M. (1987a). The entorhinal cortex of the monkey: II. Cortical afferents. *Journal of Comparative Neurology*, 264(3), 356–395. <https://doi.org/10.1002/cne.902640306>
- Insausti, R., Amaral, D. G., & Cowan, W. M. (1987b). The entorhinal cortex of the monkey: III. Subcortical afferents. *Journal of Comparative Neurology*, 264(3), 396–408. <https://doi.org/10.1002/cne.902640307>
- Insausti, R., Insausti, A. M., Muñoz López, M., Medina Lorenzo, I., del Mar Arroyo-Jiménez, M., Marcos Rabal, M. P., de la Rosa-Prieto, C., Delgado-González, J. C., Montón Etxeberria, J., Cebada-Sánchez, S., Raspeño-García, J. F., Iñiguez de Onzoño, M. M., Molina Romero, F. J., Benavides-Piccione, R., Tapia-González, S., Wisse, L. E. M., Ravikumar, S., Wolk, D. A., De Felipe, J., ... Artacho-Pérola, E. (2023). Ex vivo, in situ perfusion protocol for human brain fixation compatible with microscopy, MRI techniques, and anatomical studies. *Frontiers in Neuroanatomy*, 17, 1149674. <https://doi.org/10.3389/fnana.2023.1149674>
- Insausti, R., Muñoz-Lopez, M., Insausti, A. M., & Artacho-Perula, E. (2017). The human periallocortex: Layer pattern in presubiculum, parasubiculum and entorhinal cortex. A review. *Frontiers in Neuroanatomy*, 11, 84. <https://doi.org/10.3389/fnana.2017.00084>
- Joelving, F. C., Billeskov, R., Christensen, J. R., West, M., & Pakkenberg, B. (2006). Hippocampal neuron and glial cell numbers in Parkinson's disease—A stereological study. *Hippocampus*, 16(10), 826–833. <https://doi.org/10.1002/hipo.20212>
- Jones, M. W., & McHugh, T. J. (2011). Updating hippocampal representations: CA2 joins the circuit. *Trends in Neurosciences*, 34(10), 526–535. <https://doi.org/10.1016/j.tins.2011.07.007>
- Keuler, J. I., Luiten, P. G., & Fuchs, E. (2003). Preservation of hippocampal neuron numbers in aged rhesus monkeys. *Neurobiology of Aging*, 24(1), 157–165. [https://doi.org/10.1016/s0197-4580\(02\)00062-3](https://doi.org/10.1016/s0197-4580(02)00062-3)
- Kilias, A., Tulke, S., Barheier, N., Ruther, P., & Häussler, U. (2022). Integration of the CA2 region in the hippocampal network during epileptogenesis. *Hippocampus*, 33(3), 223–240. Portico. <https://doi.org/10.1002/hipo.23479>
- Kohara, K., Pignatelli, M., Rivest, A. J., Jung, H. Y., Kitamura, T., Suh, J., Frank, D., Kajikawa, K., Mise, N., Obata, Y., Wickersham, I. R., & Tonegawa, S. (2014). Cell type-specific genetic and optogenetic tools reveal hippocampal CA2 circuits. *Nature Neuroscience*, 17(2), 269–279. <https://doi.org/10.1038/nn.3614>
- Kovelman, J. A., & Scheibel, A. B. (1984). A neurohistological correlate of schizophrenia. *Biological Psychiatry*, 19(12), 1601–1621.
- Lauer, M., & Senitz, D. (2006). Dendritic excrescences seem to characterize hippocampal CA3 pyramidal neurons in humans. *Journal of Neural Transmission (Vienna)*, 113(10), 1469–1475. <https://doi.org/10.1007/s00702-005-0428-8>
- Lee, S. E., Simons, S. B., Heldt, S. A., Zhao, M., Schroeder, J. P., Vellano, C. P., Cowan, D. P., Ramineni, S., Yates, C. K., Feng, Y., Smith, Y., Sweatt, J. D., Weinschenker, D., Ressler, K. J., Dudek, S. M., &

- Hepner, J. R. (2010). RGS14 is a natural suppressor of both synaptic plasticity in CA2 neurons and hippocampal-based learning and memory. *Proceedings of the National Academy of Sciences of the United States of America*, 107(39), 16994–16998. <https://doi.org/10.1073/pnas.1005362107>
- Lein, E. S., Callaway, E. M., Albright, T. D., & Gage, F. H. (2005). Redefining the boundaries of the hippocampal CA2 subfield in the mouse using gene expression and 3-dimensional reconstruction. *The Journal of Comparative Neurology*, 485(1), 1–10. <https://doi.org/10.1002/cne.20426>
- Lein, E. S., Zhao, X., & Gage, F. H. (2004). Defining a molecular atlas of the hippocampus using DNA microarrays and high-throughput in situ hybridization. *The Journal of Neuroscience*, 24(15), 3879–3889. <https://doi.org/10.1523/JNEUROSCI.4710-03.2004>
- Lim, C., Blume, H. W., Madsen, J. R., & Saper, C. B. (1997). Connections of the hippocampal formation in humans: I. The mossy fiber pathway. *The Journal of Comparative Neurology*, 385(3), 325–351. [https://doi.org/10.1002/\(sici\)1096-9861\(19970901\)385:3<325::aid-cne1>3.0.co;2-5](https://doi.org/10.1002/(sici)1096-9861(19970901)385:3<325::aid-cne1>3.0.co;2-5)
- Lim, C., Mufson, E. J., Kordower, J. H., Blume, H. W., Madsen, J. R., & Saper, C. B. (1997). Connections of the hippocampal formation in humans: II. The endfolial fiber pathway. *The Journal of Comparative Neurology*, 385(3), 352–371.
- Lorente de Nó, R. (1934). Studies on the structure of the cerebral cortex II. Continuation of the study of the ammonic system. *Journal für Psychologie und Neurologie*, 46, 113–117.
- Magloczky, Z., Acscady, L., & Freund, T. F. (1994). Principal cells are the postsynaptic targets of supramammillary afferents in the hippocampus of the rat. *Hippocampus*, 4(3), 322–334. <https://doi.org/10.1002/hipo.450040316>
- Malchow, B., Strocka, S., Frank, F., Bernstein, H.-G., Steiner, J., Schneider-Axmann, T., Hasan, A., Reich-Erkelenz, D., Schmitz, C., Bogerts, B., Falkai, P., & Schmitt, A. (2014). Stereological investigation of the posterior hippocampus in affective disorders. *Journal of Neural Transmission*, 122(7), 1019–1033. <https://doi.org/10.1007/s00702-014-1316-x>
- Margerison, J. H., & Corsellis, J. A. (1966). Epilepsy and the temporal lobes. A clinical, electroencephalographic and neuropathological study of the brain in epilepsy, with particular reference to the temporal lobes. *Brain*, 89(3), 499–530. <https://doi.org/10.1093/brain/89.3.499>
- Mesulam, M.-M., Rosen, A. D., & Mufson, E. J. (1984). Regional variations in cortical cholinergic innervation: Chemoarchitectonics of acetylcholinesterase-containing fibers in the macaque brain. *Brain Research*, 311(2), 245–258. [https://doi.org/10.1016/0006-8993\(84\)90087-8](https://doi.org/10.1016/0006-8993(84)90087-8)
- Middleton, S. J., & McHugh, T. J. (2020). CA2: A highly connected intrahippocampal relay. *Annual Review of Neuroscience*, 43, 55–72. <https://doi.org/10.1146/annurev-neuro-080719-100343>
- Moore, R. Y., & Halaris, A. E. (1975). Hippocampal innervation by serotonin neurons of the midbrain raphe in the rat. *The Journal of Comparative Neurology*, 164(2), 171–183. <https://doi.org/10.1002/cne.901640203>
- Munoz, M., & Insausti, R. (2005). Cortical efferents of the entorhinal cortex and the adjacent parahippocampal region in the monkey (*Macaca fascicularis*). *The European Journal of Neuroscience*, 22(6), 1368–1388. <https://doi.org/10.1111/j.1460-9568.2005.04299.x>
- Nelson, P. T., Dickson, D. W., Trojanowski, J. Q., Jack, C. R., Boyle, P. A., Arfanakis, K., Rademakers, R., Alafuzoff, I., Attems, J., Brayne, C., Coyle-Gilchrist, I. T. S., Chui, H. C., Fardo, D. W., Flanagan, M. E., Halliday, G., Hokkanen, S. R. K., Hunter, S., Jicha, G. A., Katsumata, Y., ... Schneider, J. A. (2019). Limbic-predominant age-related TDP-43 encephalopathy (LATE): consensus working group report. *Brain*, 142(6), 1503–1527. <https://doi.org/10.1093/brain/awz099>
- Nitsch, R., & Leranthe, C. (1993). Calretinin immunoreactivity in the monkey hippocampal formation: II. Intrinsic GABAergic and hypothalamic non-GABAergic systems: An experimental tracing and co-existence study. *Neuroscience*, 55(3), 797–812. [https://doi.org/10.1016/0306-4522\(93\)90442-i](https://doi.org/10.1016/0306-4522(93)90442-i)
- Nitsch, R., & Leranthe, C. (1994). Substance P-containing hypothalamic afferents to the monkey hippocampus: an immunocytochemical, tracing, and coexistence study. *Experimental Brain Research*, 101(2), 231–240. <https://doi.org/10.1007/BF00228743>
- Nitsch, R., & Ohm, T. G. (1995). Calretinin immunoreactive structures in the human hippocampal formation. *The Journal of Comparative Neurology*, 360(3), 475–487. <https://doi.org/10.1002/cne.903600309>
- Ohm, T. G., Jung, E., & Schnecko, A. (1992). A subpopulation of hippocampal glial cells specific for the zinc-containing mossy fibre zone in man. *Neuroscience Letters*, 145(2), 181–184. [https://doi.org/10.1016/0304-3940\(92\)90017-2](https://doi.org/10.1016/0304-3940(92)90017-2)
- Palomero-Gallagher, N., Kedo, O., Mohlberg, H., Zilles, K., & Amunts, K. (2020). Multimodal mapping and analysis of the cyto- and receptorarchitecture of the human hippocampus. *Brain Structure & Function*, 225(3), 881–907. <https://doi.org/10.1007/s00429-019-02022-4>
- Pang, C. C., Kiecker, C., O'Brien, J. T., Noble, W., & Chang, R. C. (2019). Ammon's Horn 2 (CA2) of the hippocampus: A long-known region with a new potential role in neurodegeneration. *The Neuroscientist*, 25(2), 167–180. <https://doi.org/10.1177/1073858418778747>
- Piskrowski, R. A., & Chevaleyre, V. (2012). Synaptic integration by different dendritic compartments of hippocampal CA1 and CA2 pyramidal neurons. *Cellular and Molecular Life Sciences*, 69(1), 75–88. <https://doi.org/10.1007/s00018-011-0769-4>
- Radzicki, D., Chong, S., & Dudek, S. M. (2023). Morphological and molecular markers of mouse area CA2 along the proximodistal and dorsoventral hippocampal axes. *Hippocampus*, 33(3), 133–149. <https://doi.org/10.1002/hipo.23509>
- Ramon y Cajal, S. (1904). Textura del Sistema Nervioso del Hombre y de los Vertebrados. In *Textura del Sistema Nervioso del Hombre y de los Vertebrados* (Vol. II). Imprenta Nicolás Moya.
- Rogers Flattery, C. N., Rosen, R. F., Farberg, A. S., Dooyema, J. M., Hof, P. R., Sherwood, C. C., Walker, L. C., & Preuss, T. M. (2020a). Correction to: Quantification of neurons in the hippocampal formation of chimpanzees: comparison to rhesus monkeys and humans. *Brain Structure & Function*, 225(9), 2899–2900. <https://doi.org/10.1007/s00429-020-02156-w>
- Rogers Flattery, C. N., Rosen, R. F., Farberg, A. S., Dooyema, J. M., Hof, P. R., Sherwood, C. C., Walker, L. C., & Preuss, T. M. (2020b). Quantification of neurons in the hippocampal formation of chimpanzees: comparison to rhesus monkeys and humans. *Brain Structure & Function*, 225(8), 2521–2531. <https://doi.org/10.1007/s00429-020-02139-x>
- Rosene, D. L., & van Hoesen, G. W. (1987). The hippocampal formation in the primate brain. A review of some comparative aspects by cytoarchitecture and connections. In E. G. Jones & A. Peters (Eds.), *A cerebral cortex* (Vol. 6, pp. 345–456). Plenum Press.
- Rowland, D. C., & Moser, M. B. (2013). Time finds its place in the hippocampus. *Neuron*, 78(6), 953–954. <https://doi.org/10.1016/j.neuron.2013.05.039>
- Scharfman, H. E. (2007). The CA3 "backprojection" to the dentate gyrus. *Progress in Brain Research*, 163, 627–637. [https://doi.org/10.1016/S0079-6123\(07\)63034-9](https://doi.org/10.1016/S0079-6123(07)63034-9)
- Seress, L., Gulyas, A. I., Ferrer, I., Tunon, T., Soriano, E., & Freund, T. F. (1993). Distribution, morphological features, and synaptic connections of parvalbumin- and calbindin D28k-immunoreactive neurons in the human hippocampal formation. *The Journal of Comparative Neurology*, 337(2), 208–230. <https://doi.org/10.1002/cne.903370204>
- Seress, L., & Leranthe, C. (1996). Distribution of substance P-immunoreactive neurons and fibers in the monkey hippocampal formation. *Neuroscience*, 71(3), 633–650. [https://doi.org/10.1016/0306-4522\(95\)00465-3](https://doi.org/10.1016/0306-4522(95)00465-3)

- Shinohara, Y., Hosoya, A., Yahagi, K., Ferecsko, A. S., Yaguchi, K., Sik, A., Itakura, M., Takahashi, M., & Hirase, H. (2012). Hippocampal CA3 and CA2 have distinct bilateral innervation patterns to CA1 in rodents. *The European Journal of Neuroscience*, 35(5), 702–710. <https://doi.org/10.1111/j.1460-9568.2012.07993.x>
- Simic, G., Kostovic, I., Winblad, B., & Bogdanovic, N. (1997). Volume and number of neurons of the human hippocampal formation in normal aging and Alzheimer's disease. *The Journal of Comparative Neurology*, 379(4), 482–494. [https://doi.org/10.1002/\(sici\)1096-9861\(19970324\)379:4<482::aid-cne2>3.0.co;2-z](https://doi.org/10.1002/(sici)1096-9861(19970324)379:4<482::aid-cne2>3.0.co;2-z)
- Squires, K. E., Gerber, K. J., Pare, J. F., Branch, M. R., Smith, Y., & Hepler, J. R. (2018). Regulator of G protein signaling 14 (RGS14) is expressed pre- and postsynaptically in neurons of hippocampus, basal ganglia, and amygdala of monkey and human brain. *Brain Structure & Function*, 223(1), 233–253. <https://doi.org/10.1007/s00429-017-1487-y>
- Stephan, H. (1975). *Alloccortex*. Springer Verlag.
- Swanson, L. W., Wyss, J. M., & Cowan, W. M. (1978). An autoradiographic study of the organization of intrahippocampal association pathways in the rat. *The Journal of Comparative Neurology*, 181(4), 681–715. <https://doi.org/10.1002/cne.901810402>
- Tamamaki, N., Abe, K., & Nojo, Y. (1988). Three-dimensional analysis of the whole axonal arbors originating from single CA2 pyramidal neurons in the rat hippocampus with the aid of a computer graphic technique. *Brain Research*, 452(1–2), 255–272. [https://doi.org/10.1016/0006-8993\(88\)90030-3](https://doi.org/10.1016/0006-8993(88)90030-3)
- Veazey, R. B., Amaral, D. G., & Cowan, W. M. (1982a). The morphology and connections of the posterior hypothalamus in the cynomolgus monkey (*Macaca fascicularis*). I. Cytoarchitectonic organization. *Journal of Comparative Neurology*, 207(2), 114–134. <https://doi.org/10.1002/cne.902070203>
- Veazey, R. B., Amaral, D. G., & Cowan, W. M. (1982b). The morphology and connections of the posterior hypothalamus in the cynomolgus monkey (*Macaca fascicularis*). II. Efferent connections. *Journal of Comparative Neurology*, 207(2), 135–156. <https://doi.org/10.1002/cne.902070204>
- Vertes, R. P., & McKenna, J. T. (2000). Collateral projections from the supramammillary nucleus to the medial septum and hippocampus. *Synapse*, 38(3), 281–293. [https://doi.org/10.1002/1098-2396\(20001201\)38:3<281::AID-SYN7>3.0.CO;2-6](https://doi.org/10.1002/1098-2396(20001201)38:3<281::AID-SYN7>3.0.CO;2-6)
- Villar-Conde, S., Astillero-Lopez, V., Gonzalez-Rodriguez, M., Villanueva-Anguita, P., Saiz-Sanchez, D., Martinez-Marcos, A., Flores-Cuadrado, A., & Ubeda-Bañon, I. (2021). The human hippocampus in parkinson's disease: An integrative stereological and proteomic study. *Journal of Parkinson's Disease*, 11(3), 1345–1365. <https://doi.org/10.3233/jpd-202465>
- von Economo, C. F., & Koskinas, G.N. (1925). *Die Cytoarchitektonik der Hirnrinde des erwachsenen Menschen*. J. Springer.
- Walker, J. M., Richardson, T. E., Farrell, K., Iida, M. A., Foong, C., Shang, P., Attems, J., Ayalon, G., Beach, T. G., Bigio, E. H., Budson, A., Cairns, N. J., Corrada, M., Cortes, E., Dickson, D. W., Fischer, P., Flanagan, M. E., Franklin, E., Gearing, M., ... Cray, J. F. (2021). Early selective vulnerability of the CA2 hippocampal subfield in primary age-related tauopathy. *Journal of Neuropathology & Experimental Neurology*, 80(2), 102–111. <https://doi.org/10.1093/jnen/nlaa153>
- West, M. J. (1993). Regionally specific loss of neurons in the aging human hippocampus. *Neurobiology of Aging*, 14(4), 287–293. [https://doi.org/10.1016/0197-4580\(93\)90113-p](https://doi.org/10.1016/0197-4580(93)90113-p)
- West, M. J., & Gundersen, H. J. (1990). Unbiased stereological estimation of the number of neurons in the human hippocampus. *The Journal of Comparative Neurology*, 296(1), 1–22. <https://doi.org/10.1002/cne.902960102>
- Witter, M. P., & Amaral, D. G. (1991). Entorhinal cortex of the monkey: V. Projections to the dentate gyrus, hippocampus, and subicular complex. *The Journal of Comparative Neurology*, 307(3), 437–459. <https://doi.org/10.1002/cne.903070308>
- Yokota, O., Tsuchiya, K., Noguchi, Y., Akabane, H., Ishizu, H., Saito, Y., & Akiyama, H. (2007). Coexistence of amyotrophic lateral sclerosis and argyrophilic grain disease: a non-demented autopsy case showing circumscribed temporal atrophy and involvement of the amygdala. *Neuropathology*, 27(6), 539–550. <https://doi.org/10.1111/j.1440-1789.2007.00805.x>
- Yushkevich, P. A., Munoz Lopez, M., de Onzono, I., Martin, M. M., Ittyerah, R., Lim, S., Ravikumar, S., Bedard, M. L., Pickup, S., Liu, W., Wang, J., Hung, L. Y., Lasserre, J., Vergnet, N., Xie, L., Dong, M., Cui, S., Mccollum, L., Robinson, J. L., ... Insausti, R. (2021). Three-dimensional mapping of neurofibrillary tangle burden in the human medial temporal lobe. *Brain*, 144(9), 2784–2797. <https://doi.org/10.1093/brain/awab262>
- Zhang, L., & Hernandez, V. S. (2013). Synaptic innervation to rat hippocampus by vasopressin-immuno-positive fibres from the hypothalamic supraoptic and paraventricular nuclei. *Neuroscience*, 228, 139–162. <https://doi.org/10.1016/j.neuroscience.2012.10.010>
- Zola-Morgan, S., Squire, L., & Amaral, D. (1986). Human amnesia and the medial temporal region: enduring memory impairment following a bilateral lesion limited to field CA1 of the hippocampus. *The Journal of Neuroscience*, 6(10), 2950–2967. <https://doi.org/10.1523/jneurosci.06-10-02950.1986>

How to cite this article: Insausti, R., Muñoz-López, M., & Insausti, A. M. (2023). The CA2 hippocampal subfield in humans: A review. *Hippocampus*, 33(6), 712–729. <https://doi.org/10.1002/hipo.23547>